University of West Bohemia
Faculty of Applied Sciences
Department of Mathematics

DIPLOMA THESIS

Systems with concave-convex nonlinearities: existence and multiplicity of solutions

Supervisor: Oscar Iván Agudelo Rico, Ph.D.
Consultant: doc. Ing. Gabriela Holubová, Ph.D.

Pilsen 2023

Martin Kudláč

Declaration

I hereby declare that this Diploma thesis represents my own work which I have worked out on my own under guidance of my thesis supervisor. All sources and references used during the elaboration of this work are properly cited and listed.

Pilsen, on May 5, 2023

....

Acknowledgement

I would like to express my sincere thanks to Dr. Oscar Agudelo for all his advice, for his time, dedication and willingness walk me through the pitfalls of nonlinear functional analysis. I would also like to thank doc. Gabriela Holubová, who joined our team as a consultant and also devoted a lot of time to me, thanks to which I could further improve the work.

Abstrakt

Tato práce se zabývá okrajovou úlohou pro systém dvou obyčejných diferenciálních rovnic druhého řádu s konkávními a konvexními nelinearitami a Dirichletovými okrajovými podmínkami. Jedna z rovnic obsahuje kladný parametr λ. Cílem práce je vyšetřit existenci a násobnost netriviálních řešení úlohy na základě hodnot parametru λ. Práce nejprve prezentuje výsledky numerických experimentů, díky nimž čtenář získá představu o chování zadaného systému. Stěžejním výsledkem této části je bifurkační diagram, který vykresluje závislost počtu netriviálních řešení na hodnotách parametru λ. Ve zbytku práce jsou pak poznatky získané z numerických experimentů dokazovány analyticky. K získání výsledků je použita alternativní formulace úlohy pomocí jedné obyčejné diferenciální rovnice čtvrtého řádu s Navierovými okrajovými podmínkami. Pomocí variačních metod je nalezen omezený interval pro parametr λ tak, aby úloha měla s jistotou alespoň dvě různá netriviální řešení. V závěru práce jsou získané analytické výsledky porovnány s výsledky numerických experimentů.

Klíčová slova: okrajová úloha, parametr, systém obyčejných diferenciálních rovnic, Mountain Pass, existence a násobnost řešení, bifurkační diagram

Abstract

This paper deals with a BVP for a system which consists of two ordinary differential equations of the second order with concave and convex nonlinearities and Dirichlet boundary conditions. One of the equations contains a positive parameter λ. The aim of this work is to examine existence and multiplicity of nontrivial solutions of the system based on values of the parameter λ. The paper presents results of numerical experiments which describe the behaviour of the system. The key result of this section is a bifurcation diagram which shows dependence of multiplicity of nontrivial solutions on values of the parameter λ. In the rest of the work, we tackle rigorously several of the features revealed by the numerical experiments. For this purpose, the problem is described using a single ordinary differential equation of the fourth order with Navier boundary conditions. Using variational methods, an appropriate bounded range for λ is found such that the problem has at least two distinct nontrivial solutions. At the end of the work, the analytical results are compared with the results obtained from the numerical experiments.

Keywords: boundary value problem, parameter, system of ordinary differential equations, Mountain Pass, existence and multiplicity of solutions, bifurcation diagram

Contents

Preface

This work deals with a system of two ordinary differential equations of the second order

$$\begin{cases} -u''(x) = \lambda\,|v(x)|^{r-1}\,v(x) + |v(x)|^{p-1}\,v(x), \quad 0 < x < 1 \\ -v''(x) = |u(x)|^{q-1}\,u(x), \\ \quad u, v \geq 0, \\ \quad u(0) = u(1) = v(0) = v(1) = 0, \end{cases} \tag{$*$}$$

where $p > 1$, $q > 1$, and $r \in (0, 1)$ are fixed exponents and $\lambda > 0$ is a controlled parameter. The system $(*)$ features a concave (near the origin) and convex (at infinity) nonlinearities. This work examines a connection between existence (and multiplicity) of solutions of $(*)$ and values of the parameter λ. Systems of this type describe phenomena which occur naturally for instance in population dynamics, astrophysics or fluid dynamics. In astrophysics, similar equations have occured since 19th century and they have been used for capturing behavior of density of a gas sphere [5, 10]. Known results for the topic of the systems with concave-convex nonlinearities can be found for example in [2] (for a related single equation) and [6] (for the system $(*)$ in higher dimensions). This work brings an insight to this topic in one dimension providing wide theoretical and numerical results. We emphasize that studies of such boundary value problems in dimension one often yield more precise information. Nevertheless as far as we know, this has not been explored yet for the systems of our type. In this regard, the numerical experiments presented in this work are a novel, insightful and (we believe) versatile approach to study system $(*)$. The numerical experiments represent a generalization of ideas in [11].
Our theoretical approach is motivated by the one in [2], in contrast with the approach in [6].
Chapter 1 deals with preliminary statements used later in this work as supporting arguments in proofs. A few of the statements refer to known results in the theory of Sobolev spaces. Most of the claims are, however, formulated and proved specifically for purpose of this work.
Chapter 2 first formulates the problem $(*)$ and sets out a path for answering the question of how many solutions exist for a given value of the parameter λ. Then it provides a section with numerical experiments. This section contains a detailed description of scripts designed in Matlab specifically for this work. Briefly, the scripts treat the problem $(*)$ as an initial value problem setting $u(0) = v(0) = 0$ and values of $u'(0)$ and $v'(0)$ are left as parameters. Systematically choosing different combinations of these parameters, the scripts compute thousands of solutions of initial value problems that do not necessarily satisfy the boundary condition of $(*)$ at $x = 1$. If such solutions satisfy $u(1) = v(1) = 0$, they are considered to be solutions to the original problem $(*)$. The major results of the section about numerical experiments is a bifurcation diagram which points out reasonable choices of values of the parameter λ if we try to obtain a solution of the problem.
Results from the numerical section were then used as a starting point in the development of analytical statements in Chapter 3 which rigorously examine existence and multiplicity of solutions of $(*)$. Therefore, most of the chapter is filled with proofs of analytical claims using among others the Mountain Pass theorem and the Minimization theorem as key tools for proving existence of two distinct solutions. The claims are then utilized to prove the main theorem, which sums up all the analytical results provided in this work.

At the very end of the paper, a few paragraphs are dedicated to a comparison of the analytical and the numerical results presented in Chapters 2 and 3.

Chapter 1

Preliminaries

Throughout this work we assume that the reader is familiar with basic concepts of L^p spaces and functional analysis. This chapter mentions crucial terminology and well-known statements and furthermore, it provides a theoretical background for the following chapters.
In this chapter, unless stated otherwise, we assume $1 \le p \le +\infty$, $k \in \mathbb{N}$, and $I \subset \mathbb{R}$ is an open bounded interval.

1.1 Sobolev spaces

Definition 1.1 (Weak derivative)**.** Let $u \in L^1_{loc}(I)$. A function $v \in L^1_{loc}(I)$ is the k-th weak derivative of u if for every $\varphi \in C_0^\infty(I)$

$$\int_I u(x)\, \frac{\mathrm{d}^k \varphi(x)}{\mathrm{d}x^k}\, \mathrm{d}x = (-1)^k \int_I v(x)\, \varphi(x)\, \mathrm{d}x.$$

We denote the k-th derivative by $u^{(k)}$.

Remark 1.2. The function $u^{(k)}$ is also called the weak derivative of order k. The function φ is usually called a test function. If both weak and classical derivatives exist, they coincide. For simplicity, we denote $u' = u^{(1)}$ and $u'' = u^{(2)}$.

Definition 1.3 (Sobolev space)**.** The Sobolev space $W^{k,p}(I)$ is the space of all $u \in L^p(I)$ such that $u^{(i)} \in L^p(I)$ for any $i \in \{1, \ldots, k\}$.

Remark 1.4. It is known that the mapping

$$\|.\|_{W^{k,p}(I)} : u \mapsto \|u\|_{L^p(I)} + \sum_{i=1}^{k} \|u^{(i)}\|_{L^p(I)}$$

is a norm in $W^{k,p}(I)$.

The following theorem sums up Theorems 3.3 and 3.6 in [1], p. 60–61.

Theorem 1.5. *The Sobolev space $W^{k,p}(I)$ is Banach for any $k \in \mathbb{N}$ and $p \in [1, +\infty]$. Furthermore it is separable for $p \in [1, \infty)$ and reflexive for $p \in (1, \infty)$.*

The following definition allows us to work with homogeneous Dirichlet boundary conditions in the framework of Sobolev spaces.

Definition 1.6. Let $1 \le p < +\infty$. $W_0^{1,p}(I)$ is defined as the closure of $C_c^1(I)$ in $W^{1,p}(I)$ with respect to $\|.\|_{W^{1,p}(I)}$.

A convenient description of the space $W_0^{1,p}(I)$ is given in the following theorem.

Theorem 1.7. *Let $u \in W^{1,p}(I)$. Then $u \in W_0^{1,p}(I)$ if and only if $u = 0$ on ∂I.*

The proof of this Theorem is provided in [4], Th. 8.12, p. 217.

1.1.1 Important statements for Sobolev spaces

We also mention some important results from the theory of Sobolev spaces.
The following theorem describes a crucial property of the Sobolev functions in one dimension.

Theorem 1.8 (Continuity of the Sobolev functions in $\mathbb{R}$)**.** *Let $u \in W^{1,p}(I)$. There exists a function $\tilde{u} \in C(\bar{I})$ such that*

$$u = \tilde{u} \qquad \text{a.e. in } I$$

and for any $a, b \in \bar{I}$

$$\tilde{u}(a) - \tilde{u}(b) = \int_a^b u'(x)\, dx.$$

For the proof of Theorem 1.8, see [4], Th. 8.2, p. 204.

Remark 1.9. The following holds for any $u \in W^{k,p}(I)$:

(a) $u \in C(\bar{I})$,

(b) $u^{(i)} \in C(\bar{I})$ for any $i \in \{1, \dots, k-1\}$.

Hence $u \in C^{k-1}(\bar{I})$.

The following theorem proved in [4] (Corollary 8.10, p. 215) allows us to use the integration by parts in $W^{1,p}(I)$.

Theorem 1.10 (Integration by parts)**.** *Let $f_1,\ f_2 \in W^{1,p}(I)$ for $1 \le p \le +\infty$. Then*

$$f_1\, f_2 \in W^{1,p}(I)$$

and for any $a, b \in \bar{I}$ we have

$$\int_a^b f_1'\, f_2\, dx = f_1(a)\, f_2(a) - f_1(b)\, f_2(b) - \int_a^b f_1\, f_2'\, dx. \tag{1.1}$$

Remark 1.11. We point out that if Theorem 1.10 is used for $f_1, f_2 \in W^{1,p}(I)$ and $a, b \in \bar{I}$ such that for both of the points a, b, at least one of the function f_1, f_2 vanishes, equation (1.1) simplifies to the form

$$\int_a^b f_1'\, f_2\, \mathrm{d}x = -\int_a^b f_1\, f_2'\, \mathrm{d}x.$$

Theorem 1.12 (Morrey's inequality)**.** *Let $u \in W^{1,p}(I)$ and $1 < p \le +\infty$. Then $u \in C^{0,1-\frac{1}{p}}(\bar{I})$ and for all $x, y \in \bar{I}$,*

$$|u(x) - u(y)| \le |x - y|^{1-\frac{1}{p}}\, \|u'\|_{L^p(I)}.$$

The proof of Morrey's inequality can be found in [8], Th. 4, p. 280.
The following Remark allows us to present the result of the Morrey's inequality in a broader context.

Remark 1.13. Let us assume $I = (a, b)$, $s \in [1, \infty)$, and $u \in L^\infty(a, b)$. Since I is a bounded interval, the following estimate holds

$$\|u\|_{L^s(a,b)} = \left(\int_a^b |u|^s \mathrm{d}s \right)^{\frac{1}{s}} \leq (b-a)^{\frac{1}{s}} \|u\|_{L^\infty(a,b)}.$$

Remark 1.14 (Morrey's inequality revisited). Let us assume $I = (a, b)$.

(a) If $u \in W^{1,p}(a, b)$ and $u(x_1) = 0$ for some $x_1 \in [a, b]$, the result in Theorem 1.12 yields that $u \in L^\infty(a, b)$ and in addition

$$\|u\|_{L^\infty(a,b)} \leq (b-a)^{1-\frac{1}{p}} \|u'\|_{L^p(a,b)}. \tag{1.2}$$

(b) If $u \in W^{2,p}(a, b)$ and $u'(x_2) = 0$ for some $x_2 \in [a, b]$, then

(b1) $u' \in W^{1,p}(a, b)$ and we get (1.2) for the derivative of u, in other words, $u' \in L^\infty(a, b)$ and

$$\|u'\|_{L^\infty(a,b)} \leq (b-a)^{1-\frac{1}{p}} \|u''\|_{L^p(a,b)}; \tag{1.3}$$

(b2) Remark 1.13 gives

$$|u(x) - u(y)| \leq (b-a)^{1-\frac{1}{p}} \|u'\|_{L^p(a,b)} \leq (b-a)^{\frac{1}{p}} (b-a)^{1-\frac{1}{p}} \|u'\|_{L^\infty(a,b)} \tag{1.4}$$

and applying (1.3) for inequality (1.4), the Morrey's inequality can be further iterated as follows

$$|u(x) - u(y)| \leq (b-a)(b-a)^{1-\frac{1}{p}} \|u''\|_{L^p(a,b)}$$

for any $x, y \in [a, b]$. Thus,

$$\|u\|_{L^\infty(a,b)} \leq (b-a)^{2-\frac{1}{p}} \|u''\|_{L^p(a,b)}.$$

Theorem 1.15. *Let I be bounded and let $1 < p \leq +\infty$. Then the following embeddings are compact:*

(a) $W^{1,p}(I) \subset C(\bar{I})$,

(b) $W^{1,p}(I) \subset L^p(I)$.

For proof see [4], Th. 8.8, p. 213 and [4], Th. 9.16, p. 285.
Provided the assumptions of Theorem 1.15 are satisfied, for a bounded sequence $(u_n) \subset W^{1,p}(I)$, there exist a subsequence $(u_{n_k}) \subset (u_n)$ and $u \in W^{1,p}(I)$ such that u_{n_k} converges to u uniformly in $[a, b]$ and strongly in $L^p(I)$.

1.2 The Sobolev space $X_\gamma = W^{2,\gamma}(0,1) \cap W_0^{1,\gamma}(0,1)$

For $\gamma > 1$, let us consider the space

$$X_\gamma := W^{2,\gamma}(0,1) \cap W_0^{1,\gamma}(0,1). \tag{1.5}$$

Remark 1.16. From Theorems 1.7 and 1.8, if $u \in X_\gamma$, we know that:

- u, u', and u'' belong to the space $L^\gamma(0, 1)$;
- $u \in C^1([0, 1])$;
- $u(0) = u(1) = 0$.

Let us now describe further properties of X_γ.

Properties of X_γ

X_γ is clearly a subset of the linear vector space $W_0^{1,\gamma}(0,1)$. Consider the mapping $\|.\|_{X_\gamma} : X_\gamma \to \mathbb{R}$ defined by

$$\|v\|_{X_\gamma} := \left(\int_0^1 |v''(x)|^\gamma \,\mathrm{d}x \right)^{\frac{1}{\gamma}} .$$

Now, we show that $\left(X_\gamma, \|.\|_{X_\gamma}\right)$ is a normed space.

Clearly, for any $v \in X_\gamma$ and $k \in \mathbb{R}$, we have

$$\|v\|_{X_\gamma} \geq 0, \tag{1.6}$$

$$\|v\|_{X_\gamma} = 0 \Leftrightarrow v'' = 0 \text{ a.e. in } (0,1), \tag{1.7}$$

$$\|k\,v\|_{X_\gamma} = |k| \left(\int_0^1 |v''(x)|^\gamma \,\mathrm{d}x \right)^{\frac{1}{\gamma}} . \tag{1.8}$$

Furthermore, $v'' = 0$ if and only if $v' = const.$, i.e. v is a linear function. However, since any $v \in X_\gamma$ is zero on a boundary[1], (1.6)–(1.7) necessarily imply

$$\|v\|_{X_\gamma} \geq 0 \quad \text{and} \quad \|v\|_{X_\gamma} = 0 \Leftrightarrow v = 0 \text{ on } [0,1].$$

Finally, the Minkowski inequality in $L^\gamma(0,1)$ yields for any $u, v \in X_\gamma$,

$$\|u+v\|_{X_\gamma} \leq \|u\|_{X_\gamma} + \|v\|_{X_\gamma}. \tag{1.9}$$

Consequently, from (1.6)–(1.9), X_γ endowed with $\|.\|_{X_\gamma}$ satisfies all axioms of a normed space.

For purpose of further work, we present the following lemmas.

Lemma 1.17. *If $u \in X_\gamma$, then $u \in L^\infty(0,1)$ and*

$$\|u\|_{L^\infty(0,1)} \leq \|u\|_{X_\gamma}. \tag{1.10}$$

Moreover, for any $s \in (1,\infty]$, the linear embedding

$$\begin{aligned} &i : X_\gamma \to L^s(0,1) \\ &i(u) = u \end{aligned} \tag{1.11}$$

is continuous with $\|i\| \leq 1$.

Proof. If $u \in X_\gamma$, then from Remark 1.16 and Rolle's Theorem[2] we know the following:

- $u \in W^{2,\gamma}(0,1)$,
- $u(0) = 0 = u(1)$,
- both u and u' are continuous in $[0,1]$,
- there exists $\xi \in (0,1)$ such that $u'(\xi) = 0$.

[1]See Theorem 1.7.

[2]See [13], p. 215, Prop. 1

Using the above stated properties, we obtain (1.10) directly from Remark 1.14.
Remark 1.13 further yields

$$\|u\|_{L^s(0,1)} \le \|u\|_{X_\gamma},$$

which proves the properties of (1.11). The proof is now complete. $\square$

Lemma 1.18. *The norms* $\|.\|_{X_\gamma}$ *and* $\|.\|_{W^{2,\gamma}(0,1)}$ *are equivalent in* X_γ.

Proof. For $u \in X_\gamma$, Remarks 1.13 and 1.14 imply

$$\|u'\|_{L^\gamma(0,1)} \le \|u\|_{X_\gamma}. \tag{1.12}$$

Furthemore, from Lemma 1.17 we have

$$\|u\|_{L^\gamma(0,1)} \le \|u\|_{X_\gamma}, \tag{1.13}$$

which yields

$$\frac{1}{3}\|u\|_{W^{2,\gamma}(0,1)} \le \|u\|_{X_\gamma} \le \|u\|_{W^{2,\gamma}(0,1)}.$$

$\square$

Lemma 1.19. *Space* X_γ *is Banach for any* $\gamma > 1$.

Proof. Let us consider a Cauchy sequence $(u_n) \subset X_\gamma$, that is, for any $\varepsilon > 0$ there exists $n_0 \in \mathbb{N}$ such that for any $k, l \in \mathbb{N}$ it holds that

$$\text{if } k > n_0 \text{ and } l > n_0, \text{ we have } \|u_k - u_l\|_{X_\gamma} < \varepsilon. \tag{1.14}$$

First we prove that (u_n) is Cauchy both in $W_0^{1,\gamma}(0,1)$ and $W^{2,\gamma}(0,1)$. Let us consider k, l satisfying assumptions in (1.14). Since $u_k - u_l \in X_\gamma$, Remark 1.16 and Rolle's Theorem imply that for some $\xi \in (0,1)$, $u_k'(\xi) - u_l'(\xi) = 0$.
Therefore, Remarks 1.13 and 1.14 yield

$$\|u_k' - u_l'\|_{L^\gamma(0,1)} \le \|u_k - u_l\|_{X_\gamma}. \tag{1.15}$$

Since $\|u'\|_{L^\gamma(0,1)}$ and $\|u\|_{W^{1,\gamma}(0,1)}$ are equivalent norms in $W_0^{1,\gamma}(0,1)$ and since $k, l \in \mathbb{N}$ satisfying (1.14) were chosen arbitrarily, inequality (1.15) gives that (u_n) is Cauchy in $W_0^{1,\gamma}(0,1)$.
The sequence (u_n) is also Cauchy in $W^{2,\gamma}(0,1)$ from Lemma 1.18.

Since the spaces $W^{2,\gamma}(0,1)$ and $W_0^{1,\gamma}(0,1)$ are Banach spaces, there exist functions $\hat{u_1} \in W^{2,\gamma}(0,1)$ and $\hat{u_2} \in W_0^{1,\gamma}(0,1)$ such that

$$\|u_n - \hat{u_1}\|_{W^{2,\gamma}(0,1)} \to 0 \quad \text{and} \quad \|u_n - \hat{u_2}\|_{W_0^{1,\gamma}(0,1)} \to 0$$

as n approaches infinity.
Since for any $n \in \mathbb{N}$,

$$\|u_n - \hat{u_1}\|_{W^{1,\gamma}(0,1)} \le \|u_n - \hat{u_1}\|_{W^{2,\gamma}(0,1)},$$

$\hat{u_1} = \hat{u_2}$ a.e. in $(0,1)$.
This implies that for an arbitrary Cauchy sequence $(u_n) \subset X$, there exists $\hat{u_1} \in X_\gamma$ such that (u_n) converges to $\hat{u_1}$ strongly in X_γ. The proof is complete. $\square$

Lemma 1.20. *For any* $\gamma > 1$, *the space* X_γ *is reflexive.*

Proof. The space X_γ is a linear subspace of $W^{2,\gamma}(0,1)$, thus we can consider the operator $T : X_\gamma \to W^{2,\gamma}(0,1)$ defined by $T(u) = u$ for any $u \in X_\gamma$.
Clearly, the operator T is injective and X_γ consists of all images of T in $W^{2,\gamma}(0,1)$. Now we need to prove that X_γ is closed in $W^{2,\gamma}(0,1)$.
We know that $W^{2,\gamma}(0,1)$ endowed with $\|.\|_{W^{2,\gamma}(0,1)}$ and X_γ endowed with $\|.\|_{X_\gamma}$ are Banach spaces[3].
Since $\|.\|_{W^{2,\gamma}(0,1)}$ and $\|.\|_{X_\gamma}$ are equivalent (see Lemma 1.18) in X_γ, we have that

$$(X_\gamma, \|.\|_{W^{2,\gamma}(0,1)})$$

is also a Banach space.
X_γ is then closed in $W^{2,\gamma}(0,1)$ and hence ([4], Prop. 3.20) yields that the space X_γ is reflexive. □

[3] See Theorem 1.5 and Lemma 1.19.

Chapter 2

An elliptic system with concave-convex nonlinearities

Let p, q, r, λ be real constants such that $r \in (0,1)$, $p, q > 1$, $qr < 1$ and $\lambda > 0$.
Let us consider the BVP

$$\begin{cases} -u''(x) = \lambda\,|v(x)|^{r-1}\,v(x) + |v(x)|^{p-1}\,v(x), \quad 0 < x < 1 \\ -v''(x) = |u(x)|^{q-1}\,u(x), \\ \quad u, v \geq 0, \\ \quad u(0) = u(1) = v(0) = v(1) = 0. \end{cases} \tag{2.1}$$

In this chapter, we examine existence and multiplicity of nontrivial non-negative solutions of (2.1) and their dependence on λ.

2.1 Formulation

To be able to work with the problem in a slightly simpler way, we rewrite the BVP (2.1) as follows

$$\begin{cases} -u''(x) = \lambda\,(v_+(x))^r + (v_+(x))^p, \quad 0 < x < 1 \\ -v''(x) = |u(x)|^{q-1}\,u(x), \\ \quad u(0) = u(1) = v(0) = v(1) = 0, \end{cases} \tag{2.2}$$

where v_+ denotes a positive part of function v, in other words for any $x \in (0,1)$

$$v_+(x) = \max\{v(x), 0\}.$$

Observe that if u, v are classical solutions of (2.2), that is $u, v \in C^2(0,1) \cap C([0,1])$ satisfy (2.2) pointwise, from the first equation, u is concave in $[0,1]$. Since $u(0) = u(1) = 0$, u is positive in $(0,1)$. Arguing in a similar manner with the second equation, the same holds for v.
Therefore, any classical solution of (2.2) is automatically positive and hence it is also a solution of (2.1).

Being u a classical smooth solution in $(0,1)$, from the second equation in (2.2) we have

$$u = -|v''|^{\frac{1}{q}-1}\,v'' \in C^2(0,1). \tag{2.3}$$

Plugging (2.3) into the first equation in (2.2) yields

$$\frac{\mathrm{d}^2}{\mathrm{d}x^2}\left(|v''(x)|^{\frac{1}{q}-1}\, v''(x)\right) = \lambda\,(v_+(x))^r + (v_+(x))^p, \quad x \in (0,1), \tag{2.4}$$

with the Navier boundary conditions

$$v(0) = v(1) = 0 = v''(0) = v''(1). \tag{2.5}$$

In this context, it is reasonable to say that a classical solution of (2.4)–(2.5) is a function $v \in C^2(0,1)$ such that $|v''(x)|^{\frac{1}{q}-1}\, v''(x)$ belongs to $C^2(0,1)$ and (2.4)–(2.5) is satisfied pointwise. This definition is rather restrictive for further study. For this reason, in this work we approach the problem in a "weaker" sense.

Set $\gamma := \frac{q+1}{q}$ and let $X := X_\gamma$ be the space introduced in (1.5). Let us multiply (2.4) by an arbitrary test function $\varphi \in X$ and integrate the equation over the interval $(0,1)$.
On the left-hand side, let us carry out integration by parts. Since $\varphi(0) = \varphi(1) = 0$ (we recall that any function in X is zero at the boundary in view of Remark 1.16), we get

$$-\int_0^1 \frac{\mathrm{d}}{\mathrm{d}x}\left(|v''(x)|^{\frac{1}{q}-1}\, v''(x)\right)\, \varphi'(x)\mathrm{d}x = \int_0^1 \left(\lambda\,(v_+(x))^r\, \varphi(x) + (v_+(x))^p\, \varphi(x)\right)\mathrm{d}x.$$

Applying integration by parts again and using (2.5), we have

$$\int_0^1 |v''(x)|^{\frac{1}{q}-1}\, v''(x)\, \varphi''(x)\mathrm{d}x = \int_0^1 \left(\lambda\,(v_+(x))^r\, \varphi(x) + (v_+(x))^p\, \varphi(x)\right)\mathrm{d}x. \tag{2.6}$$

For relation (2.6) to make sense, it is enough to have integrable integrands on both sides of (2.6). In contrast with the concept of the classical solution of (2.4)–(2.5), neither we require higher order differentiability, nor we need pointwise equality of the original terms. The previous dicussions motivate the following definition.

Definition 2.1. A function $v \in X$ satisfying (2.6) for any arbitrary $\varphi \in X$ is called a weak solution of (2.4)–(2.5).

Looking for weak solutions of (2.4)–(2.5) allows us to use the *variational approach*, which is a more convenient tool for our purposes. As it was discussed above, any classical solution of (2.4)–(2.5) is a weak solution of (2.4)–(2.5). In the following proposition, we prove that, having found a weak solution of (2.4)–(2.5), it corresponds also to a classical solution of (2.4)–(2.5). Proof of the proposition is motivated by arguments presented in [9].

Proposition 2.2 (Regularity of weak solutions). *If $v \in X$ is a weak solution of (2.4)–(2.5), then the function v is also a classical solution of (2.4)–(2.5).*

Proof. To make the notation in this proof concise, we denote

$$a_2(x) = |v''(x)|^{\frac{1}{q}-1}\, v''(x) \quad \text{and} \quad a_0(x) = \lambda(v_+(x))^r + (v_+(x))^p.$$

Thus, (2.4)–(2.5) reads as

$$\begin{cases} a_2''(x) = a_0(x), \quad x \in (0,1), \\ v(0) = v(1) = v''(0) = v''(1) = 0, \end{cases} \tag{2.7}$$

whereas equation (2.6) can be rewritten as follows

$$\int_0^1 a_2(x)\,\varphi''(x)\,\mathrm{d}x = \int_0^1 a_0(x)\,\varphi(x)\mathrm{d}x \quad \forall \varphi \in X. \tag{2.8}$$

Let $v \in X$ satisfy (2.8). We need to show that

(i) $v \in C^2(0,1)$,

(ii) $a_2 \in C^2(0,1)$,

(iii) (2.7) holds pointwise.

Clearly, from Theorem 1.8, a_0 is continuous. By means of Theorem 1.10, we may integrate by parts[1] the right-hand side in (2.8) to find that

$$\int_0^1 a_2(x)\,\varphi''(x)\,\mathrm{d}x = -\int_0^1 \left(\int_0^x a_0(t)\,\mathrm{d}t\right) \varphi'(x)\,\mathrm{d}x \quad \forall \varphi \in X. \tag{2.9}$$

The integration by parts can be carried out once again, which results in

$$\int_0^1 a_2(x)\,\varphi''(x)\,\mathrm{d}x = \int_0^1 \left(\int_0^x \int_0^y a_0(t)\,\mathrm{d}t\,\mathrm{d}y\right) \varphi''(x)\,\mathrm{d}x - \left(\int_0^1 \int_0^y a_0\,\mathrm{d}t\,\mathrm{d}y\right) \varphi'(1) \quad \forall \varphi \in X,$$

or in simplified notation

$$\int_0^1 M(x)\,\varphi''(x)\,\mathrm{d}x = -\left(\int_0^1 \int_0^y a_0\,\mathrm{d}t\,\mathrm{d}y\right) \varphi'(1) \quad \forall \varphi \in X \tag{2.10}$$

with $M(x) := a_2(x) - \int_0^x \int_0^y a_0(t)\,\mathrm{d}t\,\mathrm{d}y$ for $x \in (0,1)$.

We will prove that M is a linear function and, consequently, it is twice continuosly differentiable. To begin with, we choose a concrete test function φ in (2.10). Define

$$\tilde{\varphi}(x) := \int_0^x \int_0^y M(t)\,\mathrm{d}t\,\mathrm{d}y - \frac{\mathrm{A}x^3}{6} + \mathrm{B}x, \tag{2.11}$$

where A, B are defined as

$$\begin{aligned} \mathrm{A} &:= 3\int_0^1 M(x)\,\mathrm{d}x - 3\int_0^1 \int_0^x M(t)\,\mathrm{d}t\,\mathrm{d}x, \\ \mathrm{B} &:= \tfrac{1}{2}\int_0^1 M(x)\,\mathrm{d}x - \tfrac{3}{2}\int_0^1 \int_0^x M(t)\,\mathrm{d}t\,\mathrm{d}x. \end{aligned}$$

[1] In (1.1), take $f_1(x) = \int_0^x a_0(t)\ \mathrm{d}t$ and assume f_2 is any $\varphi \in X$.

From (2.11), we directly get

$$\begin{aligned}\tilde{\varphi}'(x) &= \int\limits_0^x M(t)\,\mathrm{d}t - \frac{\mathrm{A}x^2}{2} + \mathrm{B},\\ \tilde{\varphi}''(x) &= M(x) - \mathrm{A}x.\end{aligned}$$

We now verify that $\tilde{\varphi}$ represents an admissible test function. It is easy to see that

$$\tilde{\varphi}(0) = \tilde{\varphi}(1) = 0.$$

Since $v \in X$, we know that $v'' \in L^{\frac{q+1}{q}}$. Moreover since $q > 1$, we have $L^{\frac{q+1}{q}}(0,1) \hookrightarrow L^{\frac{q+1}{q^2}}(0,1)$ and thus

$$\|a_2\|^{\frac{q+1}{q}}_{L^{\frac{q+1}{q}}(0,1)} = \int\limits_0^1 |v''|^{\frac{q+1}{q^2}}\,\mathrm{d}x \le C\,\|v''\|^{\frac{q+1}{q^2}}_{L^{\frac{q+1}{q}}(0,1)} < +\infty,$$

C is a positive constant. Therefore

$$\tilde{\varphi}'' \in L^{\frac{q+1}{q}}(0,1),$$

in other words, $\tilde{\varphi} \in X$. Moreover, $\tilde{\varphi}'(1) = 0$ and it follows from (2.10) that

$$\int\limits_0^1 M(x)\,\tilde{\varphi}''(x)\,\mathrm{d}x = 0. \tag{2.12}$$

Furthermore, using assertion (2.12) and integration by parts (Theorem 1.10),

$$\begin{aligned}\int\limits_0^1 (M(x) - Ax)^2\,\mathrm{d}x &= \int\limits_0^1 M(x)\,\tilde{\varphi}''(x)\,\mathrm{d}x - \int\limits_0^1 Ax\,\tilde{\varphi}''(x)\,\mathrm{d}x\\ &= \int\limits_0^1 A\,\tilde{\varphi}'(x)\,\mathrm{d}x = 0.\end{aligned}$$

Necessarily from the last equality, we have that $M(x) = Ax$ a.e. in $(0,1)$, in other words,

$$a_2(x) = Ax + \int\limits_0^x \int\limits_0^y a_0(t)\,\mathrm{d}t\,\mathrm{d}x \quad \text{a.e. in } (0,1), \tag{2.13}$$

which (due to differentiability of the right-hand side) yields

$$a_2 \in C^2(0,1), \quad v \in C^2(0,1), \tag{2.14}$$

which proves (i), (ii) on page 11.

It remains to be proved that v satisfies (2.7) pointwise. Differentiating twice both sides of (2.13) for $x \in (0,1)$,

$$a_2''(x) = a_0(x), \quad x \in (0,1). \tag{2.15}$$

Since $v \in X$, in view of Theorem 1.7, we have

$$v(0) = v(1) = 0. \tag{2.16}$$

Finally, we prove that v'' vanishes at the boundary. Using (2.14) and integrating by parts twice[2] the left-hand side in (2.8),

$$\int_0^1 \left(a_2'' - a_0\right)\, \varphi \,\mathrm{d}x = a_2(0)\, \varphi'(0) - a_2(1)\, \varphi'(1) \quad \forall \varphi \in X.$$

Using (2.15) then yields

$$a_2(0)\, \varphi'(0) - a_2(1)\, \varphi'(1) = 0 \quad \forall \varphi \in X.$$

Since $\varphi \in X$ is arbitrary in the last equation, necessarily $a_2(0) = a_2(1) = 0$ and hence

$$v''(0) = v''(1) = 0. \tag{2.17}$$

Assertions (2.14)–(2.17) conclude the proof of (iii) on page 11 and this completes the proof of the proposition. □

Consider the functional $J : X \to \mathbb{R}$ defined by

$$J(v) := \frac{q}{q+1} \int_0^1 |v''(x)|^{\frac{q+1}{q}} \,\mathrm{d}x - \frac{1}{r+1} \int_0^1 \lambda\, v_+^{r+1}(x) \,\mathrm{d}x - \frac{1}{p+1} \int_0^1 v_+^{p+1}(x) \,\mathrm{d}x.$$

For convenience, we can rewrite $J(v)$ as

$$J(v) = \frac{q}{q+1} \|v\|_X^{\frac{q+1}{q}} - \frac{\lambda}{r+1} \|v_+\|_{L^{r+1}(0,1)}^{r+1} - \frac{1}{p+1} \|v_+\|_{L^{p+1}(0,1)}^{p+1}. \tag{2.18}$$

From Lemma 1.17, J is well-defined.
If we examine the Gateaux derivative of J at $v \in X$ in the direction $\varphi \in X$, we get

$$DJ(v)\varphi = \int_0^1 |v''(x)|^{\frac{1}{q}-1}\, v''(x)\, \varphi'' \mathrm{d}x - \int_0^1 \left(\lambda\, |v_+(x)|^{r-1}\, v(x)\, \varphi + |v_+(x)|^{p-1}\, v(x)\, \varphi\right) \mathrm{d}x. \tag{2.19}$$

As a corollary of the Hölder's inequality, Lemma 1.17, and the preceeding remarks, for any $v, \varphi \in X$, $DJ(v)\varphi$ is well-defined (for details see (3.2) on page 22).
Also, $DJ(v)\varphi = 0$ if and only if v satisfies (2.6), i.e., v is a weak solution of (2.4)–(2.5).

* * *

Our aim now is to examine multiplicity of solutions of (2.4)–(2.5) (or (2.1), respectively) with respect to a given value of the parameter λ. The main result in this regard is concluded in the following statement.

Main Theorem. *There exists a positive constant λ_0 such that, for $\lambda \in (0, \lambda_0)$, there exist two distinct nontrivial non-negative classical solutions of (2.1).*

To prove this theorem, we proceed in a few steps. First, we get insight and intuition using numerical experiments. Second, based on the observations, we use two variational theorems (the Mountain Pass Theorem and the Minimization Theorem) to obtain two solutions for a specific range of values of the parameter λ. Finally, we verify that the solutions have the desired properties and we carry out the proof of Main Theorem.

[2] We integrate by parts by means of Theorem 1.10. First we consider $f_1 = \varphi'$, $f_2 = a_2$, subsequently $f_1 = \varphi$, $f_2 = a_2'$. Observe that $\varphi(0) = \varphi(1) = 0$, which simplifies the result.

2.2 Numerical experiments

In this section, we describe an idea we developed to obtain numerical observations for problem (2.2).[3] However, for the purpose of the numerical experiments, we have to consider a different representation of the problem.
Consider the initial value problem

$$\begin{cases} u'(x) = w(x), \quad x \geq 0 \\ w'(x) = -\lambda\,(v_+(x))^r - (v_+(x))^p, \\ v'(x) = z(x), \\ z'(x) = -|u(x)|^{q-1}\,u(x), \\ u(0) = 0,\ w(0) = du_0, \\ v(0) = 0,\ z(0) = dv_0, \end{cases} \tag{2.20}$$

where du_0 and dv_0 are considered as additional real parameters of the problem.
Let us suppose that (u, w, v, z) is a solution to (2.20), then the functions u and v automatically satisfy the equations and the left Dirichlet boundary conditions in (2.2). It remains to verify that u and v are zero at the right boundary (namely, at $x = 1$).
Naturally, choosing different parameters (du_0, dv_0), we compute different solutions of the corresponding problem (2.20). At the same time, when we obtain functions u and v, we can easily calculate the values $u(1)$ and $v(1)$. Hence, for certain values of du_0, dv_0, the corresponding pair of functions (u, v) becomes a solution to (2.2), whenever $u(1) = v(1) = 0$ and $u, v > 0$ in $(0, 1)$.
During the numerical experiments, we iterate predefined values of the parameters (du_0, dv_0) and compute the correspoding solutions to (2.20). When such solution satisfies

$$u(1) \approx 0,\ v(1) \approx 0,$$

in other words $|u(1)|$ and $|v(1)|$ are sufficiently small, we call (u, v) a solution to the original problem (2.2).
A reader can imagine the process as a *footballer's kick*. Two footballers kick a ball from the ground (zero height) on the left border of the field with a given initial slope. The trajectory of the kicked balls are controlled by our equations. The footballers aim at a bin located on the right border of the field. To hit the bin with a ball, it is necessary to choose the initial slope of the kick such that the ball descends to a zero height exactly on the right border of the field, neither closer, nor farther from the footballer. Since each of the footballers kicks with different strength, generally speaking, the required slopes for the one and the other footballer differ.
The implementation of this idea is described in the following subsection.

2.2.1 The implementation

We implemented the idea of the experiments as a set of scripts in Matlab. The script is optimized to provide the results in reasonable time and accuracy.

<**numerical.m**>
Define algorithm settings and values of the parameters p, q, r.
Define the initial range for du_0 and dv_0.
Define the range for the parameter λ.
Iterate through the range for λ and do the following:

[3] It suffices to consider (2.2) as described at the beginning of this chapter.

<for cycle>

Run *shooting.m* with desired settings.

<shooting.m>

Represent $du_0 - dv_0$ plane by coarse ($\Delta = 0.1$) and dense ($\Delta = 0.005$) grids.[4]

Iterate vertices of the coarse grid and run *shootandsolve.m.*

<shootandsolve.m>

Run *ode45.m* (Runge-Kutta method for ODEs from Matlab library) for (2.20) and any given initial condition $(u(0), w(0), v(0), z(0)) = (0, du_0, 0, dv_0)$.

Compute the solution and calculate the residues $u(1)$ and $v(1)$.

Return the residues as the return value.

</shootandsolve.m>

Based on the residues for a pair (du_0, dv_0), assign the pair a color using the following scheme:

- $u(1) > 0$, $v(1) > 0$ – green,
- $u(1) > 0$, $v(1) < 0$ – yellow,
- $u(1) < 0$, $v(1) > 0$ – blue,
- $u(1) < 0$, $v(1) < 0$ – red.

Plot the colors in a $du_0 - dv_0$ diagram and save them into a variable for the coarse grid.

The pair (du_0, dv_0) such that (u, v) is also a solution of (2.2) can be located exactly at the point where all colors meet, in other words, where both residues are zero.

Iterate through the vertices of the coarse grid and choose only the points which have a neighbour of a different color (we target edges between two colors).

In the dense grid, proceed only with the vertices corresponding to the chosen points in the coarse grid.

Run *shootandsolve.m* for the vertices in the dense grid.

Plot the colors in the $du_0 - dv_0$ diagram and save them into a variable for the dense grid.

Explore neighbourhood of the points in the dense grid and check whether all colors are present in the neighbourhood (if so, assume there is a solution in the neighbourhood).

Approximate the values of (du_0, dv_0) corresponding to the solution – denote them by $(solU, solV)$ – and mark them in the graph with a black circle.

Return $(solU, solV)$ – or *(Inf, Inf)* if no solution was found.

</shooting.m>

If the return value is *(Inf, Inf)* (solution not found), exit the for cycle.

Run *showsolution.m*, pass $(solU, solV)$ as a parameter.

<showsolution.m>

Compute the solution using $(solU, solV)$ and *ode45.m.*

Plot the solution (for plotting, consider the merged equation (2.4)).

Return magnitude of the plotted function.

Note: The notion of magnitude represents the norm $\|f\| = \max_{x\in[0,1]} f(x)$.

[4]The grid is uniform, square, and the distance between two neighboring vertices is Δ (in both directions du_0 and dv_0). The results are computed only in the vertices of the grid. For instance, if we consider $du_0 \in [a, b]$ and $dv_0 \in [c, d]$, the corresponding grid consists of vertices

$$\left\{(a + i\,\Delta, b + j\,\Delta) \in [a, b] \times [c, d] : \quad i = 0, 1, \ldots, \frac{b-a}{\Delta},\ j = 0, 1, \ldots, \frac{d-c}{\Delta}\right\}.$$

For simplicity, we assume $b - a, d - c, \Delta^{-1} \in \mathbb{N}$. Thus, for any unit square in $du_0 - dv_0$ plane, the coarse grid contains 10^2 vertices and the dense grid contains 200^2 vertices.

</showsolution.m>

Save the value of λ and the corresponding magnitude into a text file.

Considering the development of the results for the previous values of λ, automatically adapt the ranges of du_0 and dv_0 for the next iteration (for the optimization, it is necessary to use the narrowest range of the parameters as possible).

</for cycle>

Load results for the whole range of λ from the text file.

Vizualize dependancy of the magnitude of the solution on the parameter λ – plot the bifurcation diagram.

</numerical.m>

Using two grids in the implementation saves significant amount of time and memory. In the graph, the optimized script skips parts of the domain where the results cannot be located (from the coarse grid's point of view), thus the script leaves blank rectangles in the graph.

2.2.2 Results of the numerical experiments

As an illustration of the numerical experiments, we include results for a few values of λ. In this subsection, we consider $p = 3$, $q = 1.5$, and $r = \frac{1}{3}$.
Obviously, setting $(du_0, dv_0) = (0, 0)$ yields a trivial solution. Nevertheless, for small positive values of λ, the numerical experiments anticipate existence of a nontrivial solution as it can be seen in Figure 2.1.

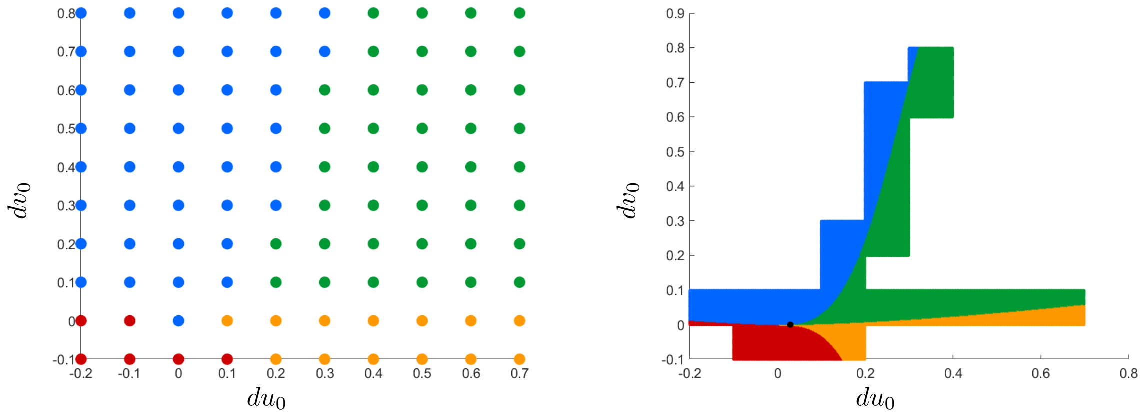

(a) Diagram for $\lambda = 1$ (coarse grid).

(b) Diagram for $\lambda = 1$ (dense grid).

Fig. 2.1: The du_0-dv_0 diagram for $\lambda = 1$ and both coarse and dense grid.

In Figure 2.1b, the experiments suggest that there exists a narrow red protrusion coming from the red area at the bottom-left corner of the diagram. At the point where it touches the green area, all four colors connect at the pair (du_0, dv_0) corresponding to a nontrivial solution.
As the value of λ increases, the red protrusion is visible for higher and higher values of du_0 and dv_0, as shown in Figure 2.2.
If we fix $\lambda = 10$, besides the solution ilustrated in Figure 2.2 with $du_0 \approx 1$ and $dv_0 \approx 0.03$, the experiments found another solution for $du_0 \approx 44$, $dv_0 \approx 16.5$, as illustrated in Figure 2.3. Figure 2.4 manifests that the magnitude of the solution for lower initial slopes du_0, dv_0 (corresponding to the

diagram in Figure 2.2) is lower than the magnitude of the other solution. Fixing $\lambda = 1$ yields similar scenario.

This suggests there exist two branches in the bifurcation diagram; the *lower branch* (closer to the trivial solution – in the view of the magnitude) and the *upper branch* (farther from the trivial solution). Based on the presented results, the branches are also getting closer to each other with increasing λ, presumably colliding at some point of bifurcation.

With this assumption, we let the script explore the range $1 \leq \lambda \leq 50$. The results confirmed the assumptions that the branches meet at some point $\tilde{\lambda} \approx 49$. Beyond $\tilde{\lambda}$, no solutions could be found. This behavior is concluded in the bifurcation diagram presented in Figure 2.5.

For $\lambda \approx \tilde{\lambda}$, it is not possible to sufficiently describe the geometry of the $du_0 - dv_0$ diagrams using the predefined grids (the red and green protrusions in the diagram are too narrow). Due to this fact, the script cannot determine the value $\tilde{\lambda}$ more accurately. Using denser grids would allow us to determine the value $\tilde{\lambda}$ in a slightly more accurate way, nevertheless, for purpose of this work, the current estimate is precise enough. More pictures can be seen in the Appendix.

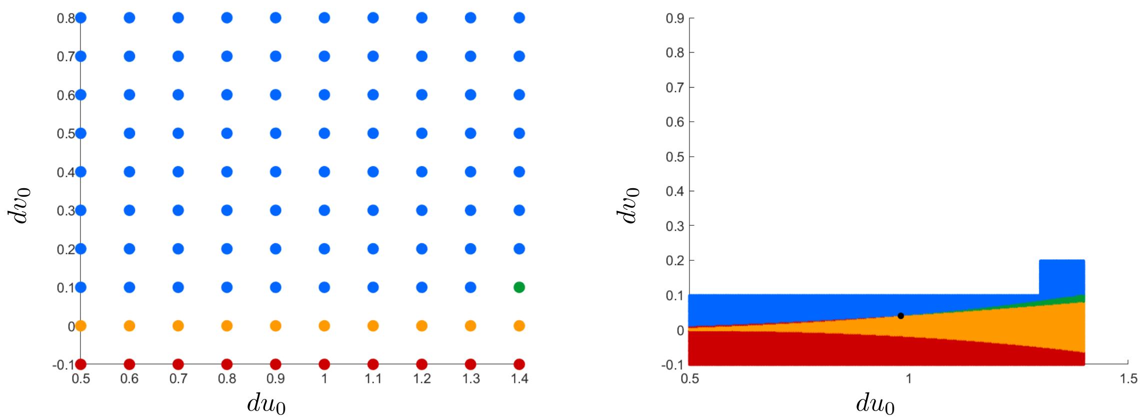

(a) Coarse grid. (b) Dense grid.

Fig. 2.2: The du_0-dv_0 diagram for $\lambda = 10$, $du_0 \approx 1$, $dv_0 \approx 0.03$

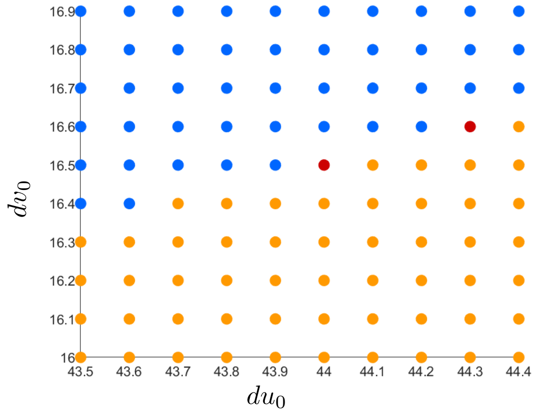

(a) Coarse grid.

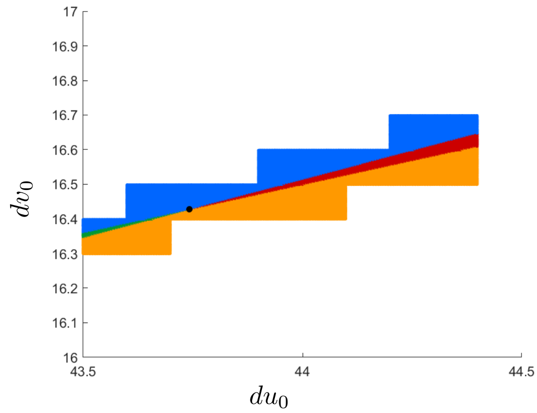

(b) Dense grid.

Fig. 2.3: The du_0-dv_0 diagram for $\lambda = 10$, $du_0 \approx 44$, $dv_0 \approx 16.5$.

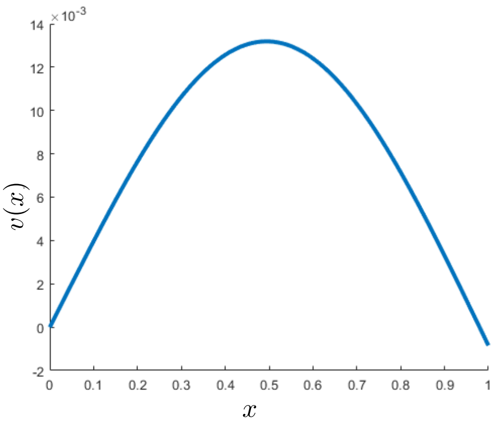

(a) Lower solution for $\lambda = 10$ corresponding to Figure 2.2.

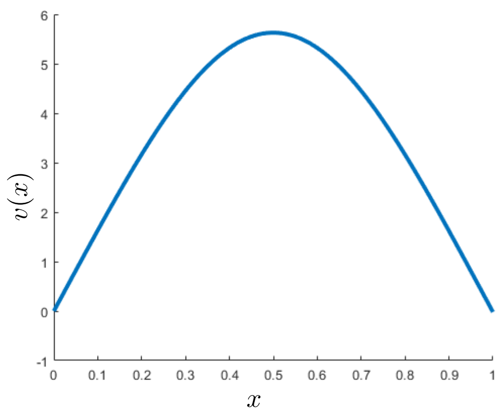

(b) Upper solution for $\lambda = 10$ corresponding to Figure 2.3.

Fig. 2.4: Comparison of two computed solutions for $\lambda = 10$.

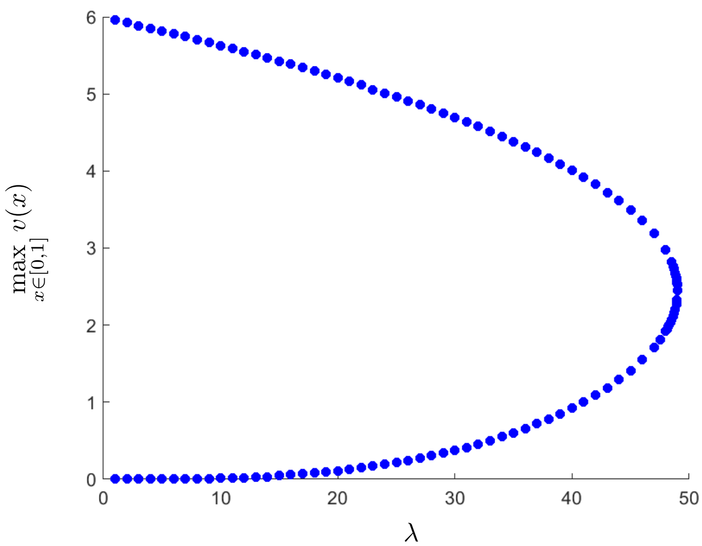

Fig. 2.5: Bifurcation diagram for the parameter λ.

2.2.3 Behavior of the energy functional

As we described above, a function $v \in X$ is a solution of (2.4)–(2.5) if and only if v is a critical point of the functional J. Thus, we might numerically examine existence of solutions by means of observing the behavior of the functional J.

Let us suppose that v is a solution to (2.4)–(2.5). For a given $\lambda > 0$, consider

$$J_{\lambda,v} : t \in \mathbb{R} \mapsto J(t\,v) \in \mathbb{R}, \tag{2.21}$$

which is a one-dimensional function capturing J in the direction[5] of v. Since v is a critical point of J, $J_{\lambda,v}$ has a critical point. We point out two important facts concerning this implication:

- We cannot reverse the implication. Generally speaking, since $J_{\lambda,v}$ captures J in a single direction and we have infinitely many linearly independent directions in X, nothing is implied by the existence of a critical point for $J_{\lambda,v}$.
- Let us suppose that the function $J_{\lambda,v}$ has a local maximum corresponding to a critical point of J. Then it does not automatically yield local maximum of J. Since we consider only a single direction, J might grow around the critical point in another directions forming a saddle point in the critical point.

From the previous numerical experiments in this section, we have a collection of solutions v for a certain set of values of λ. Based on this data, we describe $J_{\lambda,v}$ numerically in Figures 2.6, 2.7. To provide a more convenient description of the figures in relation to the bifurcation diagram in Figure 2.5, we use the following notation:

- if λ is given and v is a corresponding solution located on the upper branch in the bifurcation diagram, we denote $v^\lambda := v$,
- if λ is given and v is a corresponding solution located on the lower branch in the bifurcation diagram, we denote $v_\lambda := v$.

The horizontal axis in the figures is colored by red (green) if the function $J_{\lambda,v}$ is decreasing (increasing) at the point on the axis.

Observe that in Figure 2.6a, $J_{\lambda,v}$ has a local minimum for v_{20} and t close to zero. The experiments suggest that the functional J has a local minimum for solutions on the lower branch of the bifurcation diagram (including v_{20}). The local maximum in the figure, on the other hand, does not correspond to any critical point of J.

On contrary in Figure 2.6b, $J_{\lambda,v}$ has also a local minimum for v^{30}, but J has saddle points for solutions on the upper branch (including v^{30}), which correspond to the local maxima of J_{λ,v^λ}.

Finally in Figure 2.7, the local minimum and maximum of J_{λ,v_λ} almost meet, hence we can expect that, at the point of bifurcation, $J_{\lambda,v}$ has only an inflection point and critical points of J coincide there. For higher values of λ, no critical points of J should be present. For more pictures, see the Appendix.

In the following chapter, we attempt to confirm analytically what the numerical experiment suggest.

[5] We stress out that even though this concept looks very similar to cuts of a two-dimensional function, the situation is very different in many ways as it will be clear below. The concept only serves as an insight and has to be treated carefully.

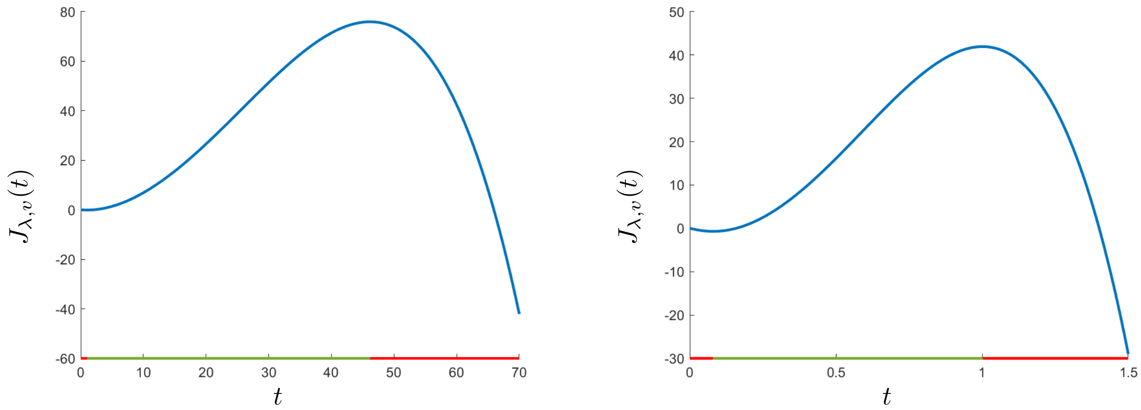

(a) J_{λ,v_λ} for $\lambda = 20$

(b) J_{λ,v^λ} for $\lambda = 30$.

Fig. 2.6: $J_{\lambda,v}$ for λ far from the point of bifurcation.

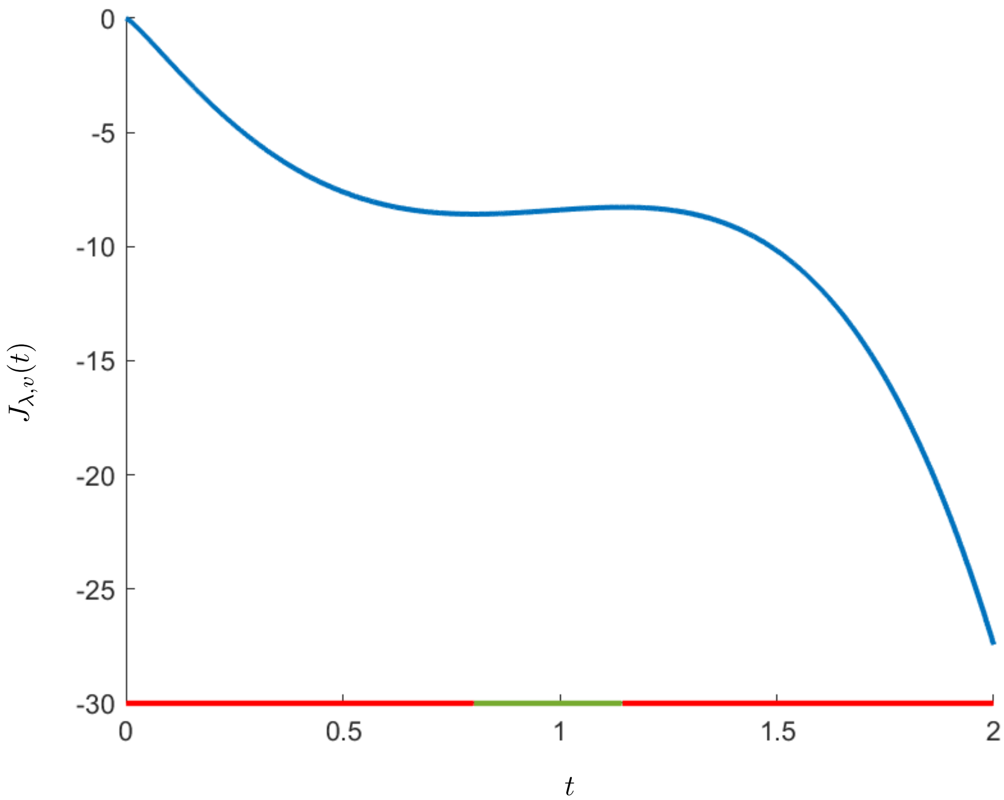

Fig. 2.7: J_{λ,v_λ} for $\lambda = 48.975$, i.e. almost at the point of bifurcation.

Chapter 3

Analytical results on existence and multiplicity of solutions

3.1 The Mountain Pass solution

We recall that, for our purpose, the problems (2.1) and (2.4)–(2.5) are equivalent. It comes straight from the formulation that (2.4)–(2.5) is always satisfied by a trivial solution for any allowed choice of the parameters p, q, r, and λ. From now on we focus only on nontrivial non-negative solutions.
The numerical experiments in Section 2.2 suggest that at least two nontrivial solutions of (2.4)–(2.5) exist. We now find the solution located on the upper branch of the bifurcation diagram (farther from the trivial solution) using the *Mountain Pass Theorem*. In what follows, X^* denotes the topological dual space of X with the topology induced by the norm in X. To clarify notations and conventions for this section, we now formulate the following statements.

Definition 3.1 (Palais-Smale condition [7])**.** Let $F \in C^1(X, \mathbb{R})$ and $c \in \mathbb{R}$. The functional F satisfies the *Palais-Smale condition on the level* c if any sequence $(u_n) \subset X$ such that

$$F(u_n) \to c, \quad \|DF(u_n)\|_{X^*} \to 0 \tag{3.1}$$

has a subsequence which converges strongly in X.

For simplicity, the Palais-Smale condition on the level c will be denoted by $(\mathrm{PS})_c$.

Theorem 3.2 (Mountain Pass Theorem [7])**.** *Let $F \in C^1(X, \mathbb{R})$, $e \in X$ and $R > 0$ be such that $\|e\| > R$ and*

$$\inf_{\substack{u \in X \\ \|u\|_X = R}} F(u) > F(o) \geq F(e).$$

If F satisfies the $(PS)_c$ condition with

$$c := \inf_{\gamma \in \Gamma} \max_{t \in [0,1]} F(\gamma(t)) \quad \textit{with} \quad \Gamma := \{\gamma \in C([0,1], X) : \gamma(0) = o, \ \gamma(1) = e\},$$

then c is a critical value of F.

Firstly we show that J satisfies the technical assumptions of Theorem 3.2.

Lemma 3.3. *The functional J belongs to $C^1(X, \mathbb{R})$.*

Proof. Let $v \in X$ be fixed, but arbitrary function. Considering the value $DJ(v)\varphi$ given by the formula (2.19), we define

$$\begin{aligned} DJ(v) : X &\to \mathbb{R} \\ \varphi &\mapsto DJ(v)\varphi. \end{aligned}$$

The mapping $DJ(v)$ is the Gateaux derivative of J at v in direction of $\varphi \in X$ if $DJ(v) \in X^*$, in other words, $DJ(v)$ is linear and bounded functional on X. Linearity of $DJ(v)$ is obvious, we now prove its boundedness.
From the triangle inequality and from properties of the integral we have

$$|DJ(v)\varphi| \leq \int_0^1 \left|(v''(x))^{\frac{1}{q}}\,\varphi''\right| \mathrm{d}x + |\lambda| \int_0^1 \left|(v_+(x))^{r-1}\,v(x)\,\varphi\right| \mathrm{d}x + \int_0^1 \left|(v_+(x))^{p-1}\,v(x)\,\varphi\right| \mathrm{d}x.$$

Using relation $v_+(x) \leq |v(x)|$ for any $x \in [0,1]$, Remarks 1.13, 1.14, Lemma 1.17, and Hölder inequality, we get

$$|DJ(v)\varphi| \leq \|v\|_X^{\frac{1}{q}}\,\|\varphi\|_X + \left(|\lambda|\,\|v\|_X^r + \|v\|_X^p\right)\|\varphi\|_X. \tag{3.2}$$

Since both λ and $v \in X$ are fixed, (3.2) yields boundedness of $DJ(v)$. Hence $DJ(v) \in X^*$ for any $v \in X$ and the Gateaux derivative of J is well-defined.

It remains to be proved that

$$\begin{aligned} DJ : X &\to X^* \\ v &\mapsto DJ(v) \end{aligned} \tag{3.3}$$

is continuous in X, that is, for any sequence $(v_n) \in X$ and any $v \in X$ such that $\|v_n - v\|_X \to 0$,

$$\sup_{\|\varphi\|_X = 1} |DJ(v_n)\varphi - DJ(v)\varphi| \to 0, \tag{3.4}$$

or to be more precise, it is enough to prove that (3.4) holds for a subsequence $(v_{n_k})_{k=1}^{+\infty} \subset (v_n)_{n=1}^{+\infty} \subset X$. We proceed in several steps.

Step 1 Preliminaries

Let us suppose we have $(v_n) \subset X$ and $v \in X$ such that $\|v_n - v\|_X \to 0$. Then Lemma 1.17 proves that $\|v_n - v\|_{L^{p+1}(0,1)} \to 0$.

Theorem 4.9 on page 94 in [4] gives a subsequence $(v_{n_k}) \subset (v_n) \subset X$ and a function $h \in L^{p+1}(0,1)$ such that

$$v_{n_k}(x) \;\to\; v(x) \text{ a.e. in } (0,1), \tag{3.5}$$

$$|v_{n_k}(x)| \;\leq\; h(x) \text{ a.e. in } (0,1) \text{ for all } k \in \mathbb{N}. \tag{3.6}$$

Since $\|v_n - v\|_X \to 0$, we have

$$\|v_{n_k} - v\|_X \to 0. \tag{3.7}$$

Let us introduce a real-valued function

$$f(s) := \lambda\, s_+^{r+1} + s_+^{p+1}$$

and for $k \in \mathbb{N}$ and any $\varphi \in X$ satisfying $\|\varphi\|_X = 1$, let us denote

$$I_1 := \int_0^1 \left| |v''_{n_k}|^{\frac{1}{q}-1} v''_{n_k} - |v''|^{\frac{1}{q}-1} v'' \right| |\varphi''| \,\mathrm{d}x,$$

$$I_2 := \int_0^1 |f(v_{n_k}(x)) - f(v(x))| \, |\varphi(x)| \,\mathrm{d}x.$$

Then, using the Triangle inequality and properties of the Lebesgue integral, we get

$$|DJ(v_{n_k})\varphi - DJ(v)\varphi| \leq I_1 + I_2. \tag{3.8}$$

We now estimate the terms I_1 and I_2 from above separately. We emphasize that, for the sake of brevity, we omit dependence on k in the notation of I_1 and I_2.

Step 2 Estimate for I_1

Since the function $|t|^{\frac{1}{q}-1}\, t$ is globally $\frac{1}{q}$−Hölder continuous, we estimate with some $C > 0$

$$I_1 \leq C \int_0^1 |v''_{n_k} - v''|^{\frac{1}{q}} \, |\varphi''| \mathrm{d}x$$

and using Hölder inequality further yields

$$I_1 \leq C \left(\int_0^1 |v''_{n_k} - v''|^{\frac{q+1}{q}} \,\mathrm{d}x \right)^{\frac{1}{q+1}} \left(\int_0^1 |\varphi''|^{\frac{q+1}{q}} \,\mathrm{d}x \right)^{\frac{q}{q+1}}$$

Since $\|\varphi\|_X = 1$, we conclude

$$I_1 \leq C \, \|v_{n_k} - v\|_X^{\frac{1}{q}}. \tag{3.9}$$

Step 3 Estimate for I_2

We demonstrate an estimate (or growth inequality) for $f(s) = \lambda s_+^{r+1} + s_+^{p+1}$ which will be used later in this proof.

If we consider $s \in \mathbb{R}$ such that $|s| \leq 1$, then

$$|f(s)| \leq \lambda + 1. \tag{3.10}$$

On the other hand, when we choose $s \in \mathbb{R}$ such that $|s| \geq 1$, then due to $r < p$, we have

$$|f(s)| = |s|^{p+1} (\lambda \, |s|^{r-p} + 1) \leq |s|^{p+1} \, (\lambda + 1). \tag{3.11}$$

Thus for any $s \in \mathbb{R}$, estimates (3.10), (3.11) give

$$|f(s)| \leq (\lambda + 1) \, (1 + |s|^{p+1}). \tag{3.12}$$

Now, we estimate I_2 from above. We use Hölder inequality, which yields

$$I_2 \leq \|f(v_{n_k}) - f(v)\|_{L^{\frac{p+1}{p}}(0,1)} \, \|\varphi\|_{L^{p+1}(0,1)} \tag{3.13}$$

and using Lemma 1.17 and the assumption $\|\varphi\|_X = 1$, inequality (3.13) reads as follows

$$I_2 \le \left(\int_0^1 |f(v_{n_k}(x)) - f(v(x))|^{\frac{p+1}{p}} \, \mathrm{d}x \right)^{\frac{p}{p+1}} . \tag{3.14}$$

We will find usefull in the following step to have also an estimate for the integrand in (3.14).

Using the convexity of the $\frac{p+1}{p}$-th power and assertion (3.12), we obtain the following estimates for all $x \in (0,1)$ and any $k \in \mathbb{N}$

$$\begin{aligned} |f(v_{n_k}(x)) - f(v(x))|^{\frac{p+1}{p}} &\le 2^{\frac{1}{p}} \left(|f(v_{n_k}(x))|^{\frac{p+1}{p}} + |f(v(x))|^{\frac{p+1}{p}} \right) \\ &\le 2^{\frac{1}{p}} (\lambda + 1) \left((1 + |v_{n_k}(x)|^p)^{\frac{p+1}{p}} + (1 + |v(x)|^p)^{\frac{p+1}{p}} \right) \\ &\le 4^{\frac{1}{p}} (\lambda + 1) \left(2 + |v_{n_k}(x)|^{p+1} + |v(x)|^{p+1} \right) . \end{aligned}$$

Finally, relation (3.6) gives for almost all $x \in (0,1)$ and $k \in \mathbb{N}$

$$|f(v_{n_k}(x)) - f(v(x))|^{\frac{p+1}{p}} \le 4^{\frac{1}{p}} (\lambda + 1) \left(2 + |h(x)|^{p+1} + |v(x)|^{p+1} \right) . \tag{3.15}$$

It is necessary to point out that, from (3.6), the function on the right-hand side of inequality (3.15) belongs to $L^1(0,1)$ from the embeddings in L^p spaces.

Step 4 Continuity of DJ

We prove that $|DJ(v_{n_k})\varphi - DJ(v)\varphi|$ converges to zero uniformly in $\varphi \in X$ with $\|\varphi\|_X = 1$. By (3.8), it is enough to prove that $I_1 \to 0$ and $I_2 \to 0$ provided $\|v_n - v\|_X \to 0$.

The convergence of I_1 follows directly from (3.7) and (3.9).

For the convergence of I_2, we use estimate (3.14) and the *Dominated Convergence Theorem.* It can be easily seen that $f(s)$ satisfies the Carathéorodory property (see [7], Def. 3.2.22, p. 136) and thus using (3.5), we get

$$|f(v_{n_k}(x)) - f(v(x))|^{\frac{p+1}{p}} \to 0 \text{ a.e. in } (0,1).$$

Moreover, the function $|f(v_{n_k}(x)) - f(v(x))|^{\frac{p+1}{p}}$ has an integrable majorant almost everywhere in $(0,1)$ (see (3.15)). Thus the Dominated Convergence Theorem gives

$$\int_0^1 |f(v_{n_k}) - f(v)|^{\frac{p+1}{p}} \mathrm{d}x \to 0$$

and hence by (3.14), $I_2 \to 0$.

The proof is now complete. □

Lemma 3.4. *The functional J satisfies $(PS)_c$ for any $c \in \mathbb{R}$.*

Proof. Let us consider a sequence $(v_n) \subset X$ satisfying (3.1) with some $c \in \mathbb{R}$. This implies that there exists $K > 0$ such that

$$J(v_n) \leq K \quad \forall n \in \mathbb{N} \tag{3.16}$$

and for any $\varepsilon > 0$ there exists $n_0 \in \mathbb{N}$ such that for all $n \in \mathbb{N}$ bigger than n_0 and for all $\varphi \in X$ we have

$$|DJ(v_n)\varphi| \leq \varepsilon \, \|\varphi\|_X. \tag{3.17}$$

First we prove that (v_n) is bounded in X. Passing to a subsequence of (v_n) (which for simplicity we denote the same), arguing by contradiction, we assume $\|v_n\|_X \to +\infty$.
Using (3.16) and (3.17), we estimate

$$K + \frac{\varepsilon}{p+1} \, \|v_n\|_X \geq J(v_n) - \frac{1}{p+1} \, DJ(v_n)v_n.$$

Lemma 1.17 yields

$$K + \frac{\varepsilon}{p+1} \, \|v_n\|_X \geq \left(\frac{q}{q+1} - \frac{1}{p+1}\right) \, \|v_n\|_X^{\frac{q+1}{q}} + \left(\frac{\lambda}{p+1} - \frac{\lambda}{r+1}\right) \, \|v_n\|_X^{r+1}. \tag{3.18}$$

Since (v_n) is not bounded, for all n sufficiently large, $\|v_n\|_X > 0$ and therefore we can divide both sides of (3.18) by $\|v_n\|_X^{\frac{q+1}{q}}$, which gives

$$\frac{K}{\|v_n\|_X^{\frac{q+1}{q}}} + \frac{\varepsilon}{(p+1)\, \|v_n\|_X^{\frac{1}{q}}} \geq \left(\frac{q}{q+1} - \frac{1}{p+1}\right) + \left(\frac{\lambda}{p+1} - \frac{\lambda}{r+1}\right) \, \frac{1}{\|v_n\|_X^{\frac{1}{q}-r}}. \tag{3.19}$$

From the assumptions for the parameters q and r, we know that all the powers of $\|v_n\|_X$ in (3.19) are positive and

$$\frac{q}{q+1} - \frac{1}{p+1} > 0.$$

Thus, taking the limit as $n \to +\infty$ in (3.19) yields a contradiction and hence (v_n) is bounded.

If we pass to a subsequence denoted for simplicity as (v_n), from Eberlain-Smulyan's Theorem (see [7], Th. 2.1.25, p. 67) and from Theorem 1.15, we have that there exists $v \in X$ such that

$$v_n \rightharpoonup v \quad \text{in } X, \tag{3.20}$$

$$v_n \to v \quad \text{in } L^{\frac{q+1}{q}}(0,1). \tag{3.21}$$

We now prove that (v_n) converges strongly in X. Since (3.20) holds and X is a uniformly convex space, it follows from [4], Prop. 3.32, p. 78, that it suffices to show that $\|v_n\|_X \to \|v\|_X$.
Denote

$$\varepsilon_n := \|DJ(v_n)\|_{X^*} := \sup_{\|\varphi\|_X = 1} |DJ(v_n)\,\varphi|.$$

Observe that $\varepsilon_n \geq 0$ and $\lim\limits_{n \to +\infty} \varepsilon_n = 0$. Choosing $\varphi := v_n - v$, (3.17) for any $n \in \mathbb{N}$ reads as

$$|DJ(v_n)\varphi| = \int_0^1 |v_n''|^{\frac{1}{q}-1} \, v_n'' \, (v_n'' - v'')\mathrm{d}x - \int_0^1 \Big(\lambda \, (v_n)_+^{r-1} \, v_n \, (v_n - v) + (v_n)_+^{p-1} \, v_n \, (v_n - v)\Big) \, \mathrm{d}x \leq$$

$$\leq \varepsilon_n \, \|\varphi\|_X.$$

Using the triangle inequality, we estimate

$$
\begin{aligned}
&\left| \int_0^1 |v_n''|^{\frac{1}{q}-1} v_n'' (v_n'' - v'') \, \mathrm{d}x \right| - \left| \int_0^1 \lambda (v_n)_+^{r-1} v_n (v_n - v) \, \mathrm{d}x \right| - \\
&\qquad - \left| \int_0^1 (v_n)_+^{p-1} v_n (v_n - v) \, \mathrm{d}x \right| \leq \varepsilon_n \, \|v_n - v\|_X .
\end{aligned} \tag{3.22}
$$

Using properties of the integral, applying $(v_n)_+^{r-1} |v_n| \leq |v_n|^r$ and the Hölder inequality for the conjugate exponents $\frac{q+1}{q}$ and $q+1$ yields

$$
\left| \int_0^1 \lambda (v_n)_+^{r-1} v_n (v_n - v) \, \mathrm{d}x \right| \leq |\lambda| \, \|v_n\|_{L^{r(q+1)}(0,1)}^r \, \|v_n - v\|_{L^{\frac{q+1}{q}}(0,1)} .
$$

Since (v_n) is a bounded sequence in X, applying Remark 1.13, Lemma 1.17, and (3.21), we obtain

$$
\lim_{n \to +\infty} \int_0^1 \lambda (v_n)_+^{r-1} v_n (v_n - v) \, \mathrm{d}x = 0. \tag{3.23}
$$

Arguing in the similar manner yields also

$$
\lim_{n \to +\infty} \int_0^1 (v_n)_+^{p-1} v_n (v_n - v) \, \mathrm{d}x = 0. \tag{3.24}
$$

We recall that (v_n) is bounded in X and $\varepsilon_n \to 0$, therefore (3.22), (3.23), and (3.24) imply

$$
\lim_{n \to +\infty} \int_0^1 |v_n''|^{\frac{1}{q}-1} v_n'' (v_n'' - v'') \, \mathrm{d}x = 0. \tag{3.25}
$$

In addition, from the definition of the weak convergence given by (3.20), we know that

$$
\lim_{n \to +\infty} \int_0^1 |v''|^{\frac{1}{q}-1} v'' (v_n'' - v'') \, \mathrm{d}x = 0 \tag{3.26}
$$

and hence subtracting terms in (3.25) and (3.26) and using Hölder inequality yields

$$
\begin{aligned}
0 &= \lim_{n \to +\infty} \left(\|v_n\|_X^{\frac{q+1}{q}} - \int_0^1 |v_n''|^{\frac{1}{q}-1} v_n'' v'' \, \mathrm{d}x - \int_0^1 |v''|^{\frac{1}{q}-1} v'' v_n'' \, \mathrm{d}x + \|v\|_X^{\frac{q+1}{q}} \right) \\
&\geq \lim_{n \to +\infty} \left(\|v_n\|_X^{\frac{q+1}{q}} - \|v_n\|_X^{\frac{1}{q}} \|v\|_X - \|v\|_X^{\frac{1}{q}} \|v_n\|_X + \|v\|_X^{\frac{q+1}{q}} \right) \\
&= \lim_{n \to +\infty} \left(\|v_n\|_X^{\frac{1}{q}} - \|v\|_X^{\frac{1}{q}} \right) \left(\|v_n\|_X - \|v\|_X \right).
\end{aligned}
$$

Since the function $x \mapsto x^{\frac{1}{q}}$ is strictly increasing,

$$
0 \geq \lim_{n \to +\infty} \left(\|v_n\|_X^{\frac{1}{q}} - \|v\|_X^{\frac{1}{q}} \right) \left(\|v_n\|_X - \|v\|_X \right) \geq 0,
$$

thus, necessarily,

$$\|v_n\|_X \to \|v\|_X. \tag{3.27}$$

Assertions (3.20) and (3.27) prove the statement. $\square$

Now we verify that J has the desired geometry described in Theorem 3.2.

Lemma 3.5. *There exist positive constants T, $\lambda_0 = \lambda_0(T,p,q,r)$ such that for all $\lambda \in (0,\lambda_0)$ there exists $C = C(T,p,q,r,\lambda)$ so that for any $v \in X$ satisfying $\|v\|_X = T$ we have $J(v) \geq C > 0$.*

Proof. Observe that for any $v \in X$ and any $s > 1$ it holds that $\|v_+\|_{L^s(0,1)} \leq \|v\|_{L^s(0,1)}$. Applying Lemma 1.17, from (2.18) we estimate

$$J(v) \geq \frac{q}{q+1}\|v\|_X^{\frac{q+1}{q}} - \frac{\lambda}{r+1}\|v\|_X^{r+1} - \frac{1}{p+1}\|v\|_X^{p+1}.$$

A trivial operation further gives

$$J(v) \geq \|v\|_X^{r+1}\left(\frac{q}{q+1}\,\|v\|_X^{\frac{1}{q}-r} - \frac{\lambda}{r+1} - \frac{1}{p+1}\,\|v\|_X^{p-r}\right). \tag{3.28}$$

Consider the function

$$h(t) := \frac{q}{q+1}\,t^{\frac{1}{q}-r} - \frac{1}{p+1}\,t^{p-r}, \quad t \geq 0,$$

then direct calculation yields

$$h'(t) = \frac{1-qr}{q+1}\,t^{\frac{1}{q}-r-1} - \frac{p-r}{p+1}\,t^{p-r-1}, \quad t > 0$$

and hence we get two possible points of local extremum

$$t_1 = 0 \quad \text{and} \quad t_2 = \left(\frac{(1-qr)(p+1)}{(q+1)(p-r)}\right)^{\frac{q}{pq-1}}.$$

Using the assumptions for the parameters p,q,r, we obtain $t_2 \in (0,1)$ and we can estimate

$$\frac{q}{q+1}\,t_2^{\frac{1}{q}-r} > \frac{q}{q+1}\,t_2^{p-r} > \frac{1}{p+1}\,t_2^{p-r}.$$

Clearly, $h(0) = 0$, $\lim\limits_{t\to+\infty} h(t) = -\infty$, and $h(t_2) > 0$ and thus t_2 is a point of global maximum of $h(t)$. We denote $T := t_2$.

Let $v \in X$ satisfy $\|v\|_X = T$. Inequality (3.28) for v now reads as

$$J(v) \geq T^{r+1}\left(h(T) - \frac{\lambda}{r+1}\right). \tag{3.29}$$

Denote

$$\lambda_0 := (r+1)\left(\frac{q}{q+1}\,T^{\frac{1}{q}-r} - \frac{1}{p+1}\,T^{p-r}\right) = (r+1)\,h(T)$$

and let $\lambda \in (0,\lambda_0)$. Setting

$$C := T^{r+1}\left(\frac{q}{q+1}\,T^{\frac{1}{q}-r} - \frac{1}{p+1}\,T^{p-r} - \frac{\lambda}{r+1}\right) = T^{r+1}\left(h(T) - \frac{\lambda}{\lambda_0}\,h(T)\right),$$

it follows from (3.29) that

$$J(v) \geq C > 0,$$

which gives the claim. $\square$

The constant T from Lemma 3.5 plays a significant role in deriving existence of the solutions. For simplicity, we introduce the following notation.

Notation 3.6. Let $B_T \subset X$ denote a closed ball centered in the origin with radius T, that is,

$$B_T = \{u \in X : \ \|u\|_X \leq T\}.$$

Lemma 3.7. *There exists $\tilde{v} \in X \setminus B_T$ such that $J(\tilde{v}) < 0$.*

Proof. Let $\varphi \in X$ be an arbitrary, but fixed function satisfying $\varphi \in \partial B_T$ and $\varphi > 0$ almost everywhere in $(0, 1)$. Then for $t > 1$

$$J(t\,\varphi) = \frac{q}{q+1}\,t^{\frac{q+1}{q}}\,\|\varphi\|_X^{\frac{q+1}{q}} - \frac{\lambda}{r+1}\,t^{r+1}\,\|\varphi\|_{L^{r+1}(0,1)}^{r+1} - \frac{1}{p+1}\,t^{p+1}\,\|\varphi\|_{L^{p+1}(0,1)}^{p+1},$$

and from the assumptions for the parameters p, q, r, λ, we have

$$\lim_{t\to+\infty} J(t\,\varphi) = -\infty.$$

Therefore for a sufficiently large $t > 1$, the function $\tilde{v} := t\,\varphi$ yields $\tilde{v} \in X \setminus B_T$ and $J(\tilde{v}) < 0$. ☐

The previous lemmas give us all the information needed for the proof of the following theorem.

Theorem 3.8. *Let $\lambda_0 > 0$ be as in Lemma 3.5. For $\lambda \in (0, \lambda_0)$, there exists a nontrivial weak solution $v_1 \in X$ of (2.4)–(2.5). Moreover, $J(v_1) > 0$.*

Proof. For the functional J we know the following:

- $J \in C^1(X, \mathbb{R})$ as it was proved in Lemma 3.3,
- $J(o) = 0$,
- for $\lambda \in (0, \lambda_0)$, $\inf\limits_{v\in\partial B_T} J(v) \geq C > 0$ from Lemma 3.5,
- existence of $e \in X \setminus B_T$ such that $J(e) < 0$ is provided in Lemma 3.7,
- J satisfies $(\mathrm{PS})_c$ for any $c \in \mathbb{R}$ as shown in Lemma 3.4.

Theorem 3.2 with $F = J$ and $R = T$ then yields the existence of $v_1 \in X$ such that

$$DJ(v_1)\varphi = 0 \quad \text{for any } \varphi \in X, \tag{3.30}$$
$$J(v_1) = c \tag{3.31}$$

with c defined in Theorem 3.2. Moreover, from the definition of c, it is clear that

$$J(v_1) = c \geq C > 0.$$

Equality (3.30) implies that v_1 is necessarily a weak solution of (2.4)–(2.5). From (3.31) we have that $J(v_1) > 0$ and hence v_1 is nontrivial. This completes the proof. ☐

3.2 Solution near the origin

From the numerical experiments, we also observe the existence of a solution near the trivial solution. To find it, we set out an appropriate bounded region containing the trivial solution. Then, we show that the functional J has a local minimum in this region and we also prove that this minimum corresponds to the nontrivial solution near the origin.
To accomplish this, we will use the following Theorem, which sums up Theorem 1.1 in [12], p. 2 and the corresponding comments.

Theorem 3.9 (Minimization Theorem [12])**.** *Let M be a topological Hausdorff space and suppose M is sequentially weakly compact and $E : M \to \mathbb{R} \cup \{+\infty\}$ is sequentially weakly lower semicontinuous. Then E is uniformly bounded from below on M and it attains its infimum.*

The statements in this section use notation and constants introduced in Lemma 3.5 and Notation 3.6. To begin with, we prove the following lemma.

Lemma 3.10. *There exists $\tilde{v} \in X \setminus \{0\}$ such that $\tilde{v} \in \operatorname{int} B_T$ and $J(\tilde{v}) < 0$.*

Proof. Let $\varphi \in X$ be an arbitrary, but fixed function satisfying $\varphi \in \partial B_T$ and $\varphi > 0$ almost everywhere in $(0,1)$.
Then for $t \in (0,1)$ and $\lambda > 0$

$$J(t\,\varphi) = \frac{q}{q+1}\, t^{\frac{q+1}{q}}\, \|\varphi\|_X^{\frac{q+1}{q}} - \frac{\lambda}{r+1}\, t^{r+1}\, \|\varphi\|_{L^{r+1}(0,1)}^{r+1} - \frac{1}{p+1}\, t^{p+1}\, \|\varphi\|_{L^{p+1}(0,1)}^{p+1},$$

which can be rewritten as

$$J(t\,\varphi) = t^{r+1} \left(\frac{q}{q+1}\, t^{\frac{1}{q}-r}\, \|\varphi\|_X^{\frac{q+1}{q}} - \frac{\lambda}{r+1}\, \|\varphi\|_{L^{r+1}(0,1)}^{r+1} - \frac{1}{p+1}\, t^{p-r}\, \|\varphi\|_{L^{p+1}(0,1)}^{p+1} \right).$$

Since $\frac{1}{q} > r > 0$, there exists $t > 0$ sufficiently small such that $J(t\,\varphi) < 0$. Finally, if we denote $\tilde{v} := t\,\varphi$, then $\tilde{v} \in B_T$ and $J(\tilde{v}) < 0$. This completes the proof of the lemma. □

Existence of the solution near the origin is then provided by the following theorem.

Theorem 3.11. *Let λ_0 be as in Lemma 3.5. For all $\lambda \in (0, \lambda_0)$, there exists a nontrivial weak solution $v_2 \in \operatorname{int} B_T$ of (2.4)–(2.5). In addition, $J(v_2) < 0$.*

Proof. Lemma 3.5 gives us the constant T such that, for all $\lambda \in (0, \lambda_0)$, $J(v)$ is positive on ∂B_T. Let $\lambda \in (0, \lambda_0)$ and consider a minimization problem for $J(v)$ with $v \in B_T$. We prove that the minimum is attained at the interior of B_T and that it is nontrivial.

Space X is reflexive[1] and thus, using Kakutani's Theorem (see [4], Theorem 3.17, p. 67), B_T is sequentially weakly compact.
Let us now show that J is sequentially weakly lower semicontinuous in B_T, that is, for any $(v_n) \subset B_T$ converging weakly to $v \in X$,[2]

$$J(v) \leq \liminf_{n\to+\infty} J(v_n).$$

Let us assume that $(v_n) \subset B_T$ converges weakly to $v \in X$. The norm $\|.\|_X$ is sequentially weakly lower semicontinuous[3] in B_T, therefore

$$\liminf_{n\to+\infty} J(v_n) \geq \frac{q}{q+1}\, \|v\|_X^{\frac{q+1}{q}} - \frac{\lambda}{r+1} \liminf_{n\to+\infty} \left(\int_0^1 (v_n)_+^{r+1}\, \mathrm{d}x \right) - \frac{1}{p+1} \liminf_{n\to+\infty} \left(\int_0^1 (v_n)_+^{p+1}\, \mathrm{d}x \right). \tag{3.32}$$

[1] See Lemma 1.20.
[2] In fact, since B_T is proved to be sequentially weakly compact, $v \in B_T$.
[3] From [4], Prop. 3.5 (iii), p. 58

For $s > 0$, let us denote

$$F_s : C([0,1]) \to \mathbb{R} \quad \text{such that} \quad F_s(u) = \int_0^1 u_+^{s+1}\,\mathrm{d}x,\ \ u \in C([0,1]).$$

In the uniform topology of $C([0,1])$, F_s is a composite functional of continuous mappings and thus the functional F_s is continuous.

Observe that X is continuously embedded in $W^{1,\frac{q+1}{q}}(0,1)$ (see estimates (1.12) and (1.13)), thus Theorem 1.15 yields

$$X \hookrightarrow\hookrightarrow C([0,1]).$$

Since $(v_n) \subset B_T$ converges weakly to $v \in B_T$, the sequence (v_n) converges uniformly to v in $[0,1]$ and therefore

$$F_s(v_n) \to F_s(v). \tag{3.33}$$

Inequality (3.32) and the continuity of F_s for $s = p$ and $s = r$ shown in (3.33) directly give that J is sequentially weakly lower semicontinuous in B_T.
Existence of $v_2 \in B_T$ such that

$$J(v_2) = \inf_{v \in B_T} J(v)$$

follows from Theorem 3.9.

Lemma 3.10 guarantees that $v_2 \in \operatorname{int} B_T$, v_2 is nontrivial, and $J(v_2) < 0$. Hence, clearly, the function v_2 is a weak solution of (2.4)–(2.5). Now the proof is complete. □

* * *

In the previous sections, we used two different variational methods to obtain a nontrivial weak solution for (2.4)–(2.5). However, these two solutions might correspond to the same function in X. We now prove Main Theorem[4] which rules this option out and which sums up the previous results.

Proof of Main Theorem. Let λ_0 be as in Lemma 3.5 and let us consider $\lambda \in (0, \lambda_0)$. Then it follows from Theorems 3.8 and 3.11 that there exist two weak nontrivial solutions $v_1, v_2 \in X$ of (2.4)–(2.5). Moreover, since $J(v_1) > 0 > J(v_2)$, the weak solutions are necessarily distinct.
Functions v_1, v_2 are classical solutions of (2.4)–(2.5) due to the regularity given by Proposition 2.2. Using relation (2.3), we get the corresponding nontrivial functions u_1, u_2 such that the pairs of functions (u_1, v_1) and (u_2, v_2) solve (2.2). As it was described on page 9, all the functions are necessarily non-negative. Hence for $\lambda \in (0, \lambda_0)$, the pairs (u_1, v_1) and (u_2, v_2) represent two distinct nontrivial non-negative classical solutions to (2.1). □

3.3 Remarks on existence and multiplicity of solutions

We close the chapter with a few comments concerning the results presented above.

[4]See p. 13.

Improvement of λ_0

Main Theorem claims that, for $\lambda \in (0, \lambda_0)$, there exist at least two distinct solutions of (2.1), in other words in the bifurcation diagram, we find at least two branches.[5] Naturally we can pose a question to what extend this λ_0 is accurate.

Section 2.2 predicts existence of two branches for $\lambda \in (0, \tilde{\lambda})$ and approximates $\tilde{\lambda} \approx 49$ (for $p = 3$, $q = 1.5$, and $r = 3^{-1}$). For the same values of the parameters,

$$\lambda_0 \approx 0.59 \ll \tilde{\lambda}.$$

Assuming numerical experiments correspond to the actual behavior of the system (2.1), the theoretical results in this chapter describe the system only on a very narrow interval.

Most of the inaccuracy is brought by Lemma 1.17, i.e. the embedding of the space X into L^p spaces. The embedding was proved very easily, however, the constant of the embedding appears to be very far from being optimal. Lemma 1.17 was used to get assertion (3.28) which helped us to prove Lemma 3.5. Lemma 3.5 then appeared in proofs of theorems which showed existence of the solutions both via Mountain Pass theorem and via Minimization theorem.

The higher the value of λ is, the less estimate (3.28) captures the behavior of the functional J. To extend the range of values of λ which our results can be proved for, it is reasonable to attempt to obtain a better constant of the embedding in Lemma 1.17.

For the embedding $X_\gamma \hookrightarrow L^\gamma(0,1)$ with $\gamma > 1$, there has to exist an optimal constant $C_{emb} > 0$ such that

$$\|u\|_{L^\gamma(0,1)} \leq C_{emb} \|u\|_{X_\gamma} \tag{3.34}$$

and such that there is no lower constant satisfying this inequality, that is

$$C_{emb}^{-1} = \inf_{\substack{u \in X_\gamma \\ u \neq 0}} \frac{\|u\|_{X_\gamma}}{\|u\|_{L^\gamma(0,1)}}. \tag{3.35}$$

Similarly to the well-known result for the Laplace operator, it can be shown that C_{emb}^{-1} corresponds to the first eigenvalue of the problem

$$\begin{cases} \dfrac{\mathrm{d}^2}{\mathrm{d}x^2}\left(|u''|^{\gamma-2} u''\right) = \lambda\, |u|^{\gamma-2} u, \quad x \in (0,1), \\ \qquad u(0) = u(1) = u''(0) = u''(1) = 0. \end{cases}$$

We do not know the exact value of the principal eigenvalue, however, in [3] there was proved an estimate

$$C_{emb} \leq K_{emb} := \frac{\left(\frac{1}{2}\right)^2}{2} \min\left\{ \left(\frac{\sqrt{\pi}\,\Gamma(\gamma)}{\Gamma(\gamma+\frac{1}{2})} - \frac{1}{\gamma}\right)^{\frac{1}{\gamma}}, \left(\frac{\sqrt{\pi}\,\Gamma(\gamma')}{\Gamma(\gamma'+\frac{1}{2})} - \frac{1}{\gamma'}\right)^{\frac{1}{\gamma'}} \right\}, \tag{3.36}$$

where $\gamma' := \frac{\gamma}{\gamma-1}$ and $\Gamma(z) := \int\limits_0^{+\infty} t^{z-1}\, e^{-t}\, \mathrm{d}t$.

When (3.36) is incorporated in deriving the estimate for J from below, we proceed as follows. For $v \in X$, the assumption $r < \frac{1}{q}$ yields

$$\|v_+\|_{L^{r+1}(0,1)} \leq \|v\|_{L^{r+1}(0,1)} \leq \|v\|_{L^{\frac{1}{q}+1}(0,1)}$$

[5] The constant λ_0 is presented in Lemma 3.5.

simply from embeddings of L^p spaces. We now apply (3.34) with $\gamma = \frac{1}{q} + 1$, thus in terms of (3.36), we obtain

$$\|v_+\|_{L^{r+1}(0,1)} \leq K_{emb} \|v\|_X. \tag{3.37}$$

Unfortunately, from the preceeding steps, it is clear that the same process cannot be used for the norm $\|v_+\|_{L^{p+1}(0,1)}$.
We now estimate from (2.18)

$$J(v) \geq \frac{q}{q+1} \|v\|_X^{\frac{q+1}{q}} - \frac{\lambda K_{emb}^{r+1}}{r+1} \|v\|_X^{r+1} - \frac{1}{p+1} \|v\|_X^{p+1},$$

or respectively,

$$J(v) \geq \|v\|_X^{r+1} \left(\frac{q}{q+1} \|v\|_X^{\frac{1}{q}-r} - \frac{\lambda K_{emb}^{r+1}}{r+1} - \frac{1}{p+1} \|v\|_X^{p-r} \right). \tag{3.38}$$

If we replace (3.28) by (3.38) in the proof of Lemma 3.5, we get the same result with[6]

$$\lambda_0 = \frac{r+1}{K_{emb}^{r+1}} \left(\frac{q}{q+1} T^{\frac{1}{q}-r} - \frac{1}{p+1} T^{p-r} \right). \tag{3.39}$$

For parameters $p = 3$, $q = 1.5$, and $r = 3^{-1}$, we can approximate

$$\lambda_0 \approx 10.78.$$

Even though the presented procedure is more sofisticated, it is still not optimal at all. The reason is that we applied the embedding $X \hookrightarrow L^{\frac{1}{q}+1}(0,1)$ for the term with L^{r+1}-norm, but the term with L^{p+1}-norm was still treated as before.
If we were able to find exact (optimal) constants both for the embeddings $X \hookrightarrow L^{r+1}(0,1)$ and $X \hookrightarrow L^{p+1}(0,1)$ (or at least sufficient estimates), the result would be even better. Yet, such estimates are not known to us.

Behavior of functional J for high values of λ

The value $\tilde{\lambda} \approx 49$ introduced in Section 2.2 approximates the upper bound of the interval where existence of two distinct solution is expected. Beyond $\tilde{\lambda}$, no solutions are anticipated. To prove existence of a solution, we used functional J (see (2.18)) – we looked for critical points of the functional which were proved to correspond to the solutions of (2.1). This was also described numerically in Section 2.2.
Now we ilustrate how the functional J behaves when λ exceeds a certain value. Let us take $u(x) = \sin \pi x$ for $x \in [0, 1]$. Naturally, the function u is not a solution to (2.4)–(2.5), but due to its properties, it can be used to obtain an intuition when examining the behavior of J.
For $s > -2$, we have

$$\int_0^1 u^{s+1}(x)\,\mathrm{d}x = \frac{\Gamma(1+\frac{s}{2})}{\sqrt{\pi}\,\Gamma(\frac{3+s}{2})}. \tag{3.40}$$

In Section 2.2, we chose a fixed λ and computed the functional J in the direction of a solution for the particular value of λ. The result was shown as an one-dimensional function $J_{\lambda,v}$ (see (2.21) for the definition). In this case, we consider the fixed function u and we observe, how J behaves when λ changes.

[6]For definition of T, see the proof of Lemma 3.5.

Using (3.40), we are able to descibe J analytically as a two-dimensional function

$$J_u : \quad \mathbb{R}^+ \times \mathbb{R}^+ \to \mathbb{R},$$
$$(t, \lambda) \mapsto J_{\lambda,u}(t).$$

The function $J_u = J_u(t, \lambda)$ is visualized in Figures 3.1 – 3.4.
From the figures, it is clearly visible that for λ small, the function $J_{\lambda,u}$ reaches a local maximum and then descends towards negative infinity. As λ attains a certain threshold, the local maximum disappears and the function falls down right from the beginning. Thus, we do expect that no critical points can be found for J for higher values of λ.

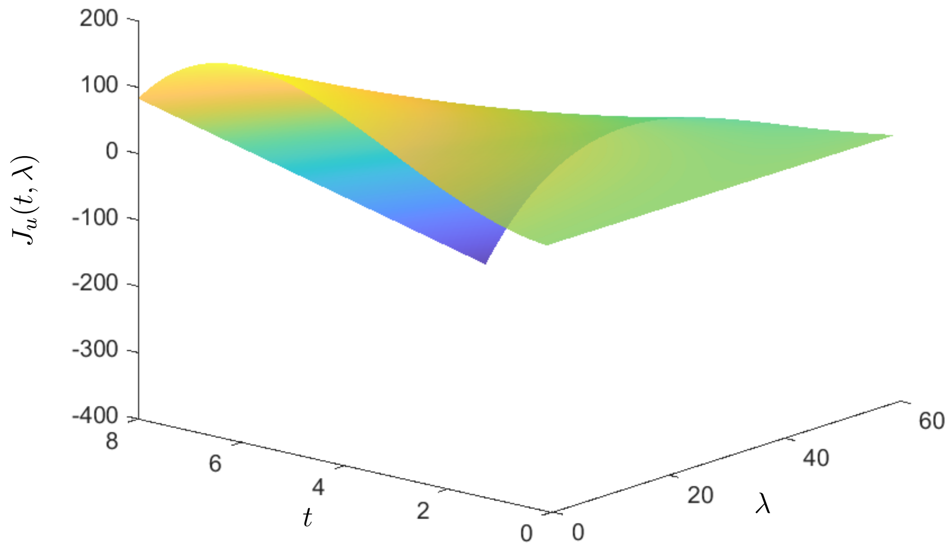

Fig. 3.1: J_u with the domain $(0, 8] \times (0, 60]$.

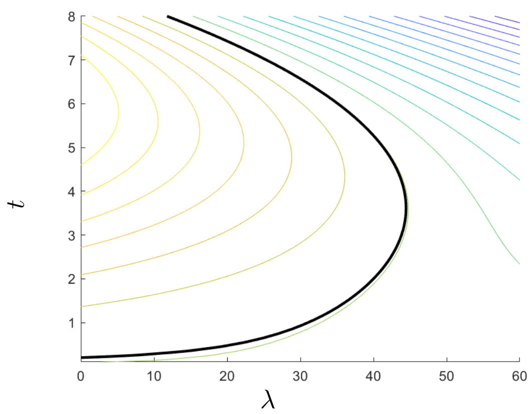

(a) Contours of J_u with highlighted level zero (black curve).

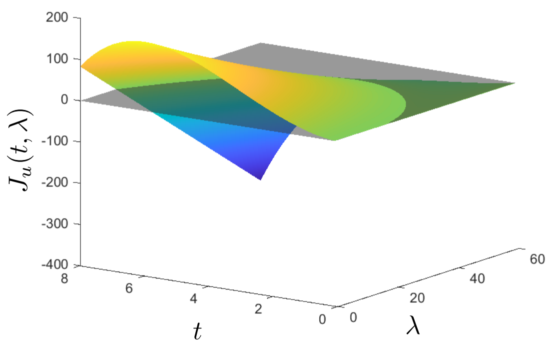

(b) Function J_u with $t\lambda$-plane (gray).

Fig. 3.2: J_u in the context of its contours.

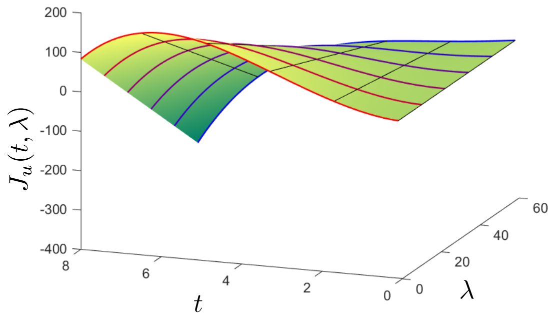

(a) Highlighted curves $J_{\lambda,u}$ for a few values of λ.

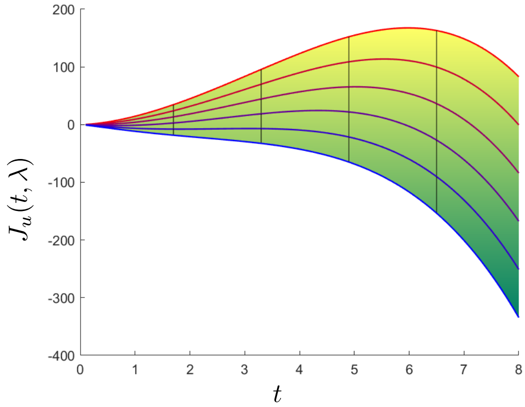

(b) Projection into tJ_u-plane.

Fig. 3.3: J_u in the context of $J_{\lambda,u}$.

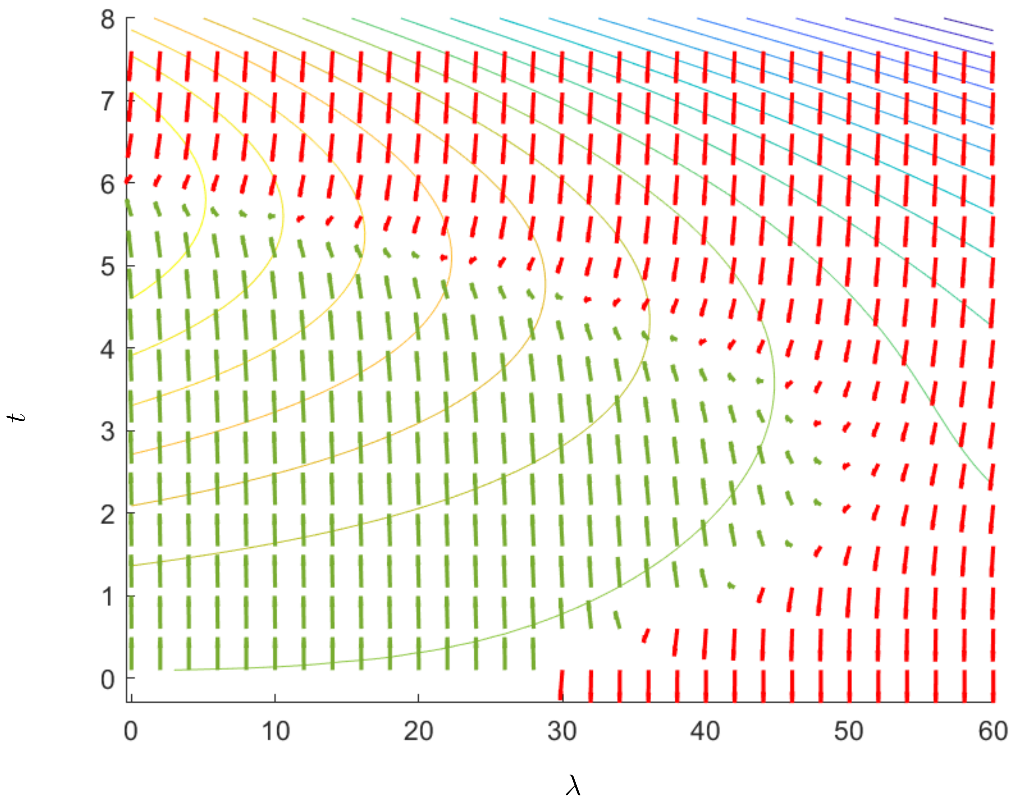

Fig. 3.4: J_u in the context of its gradient and contours. Distinguished points in the domain where $\frac{\partial J_u(t,\lambda)}{\partial t}$ is positive (green arrows) and negative (red arrows).

Appendix

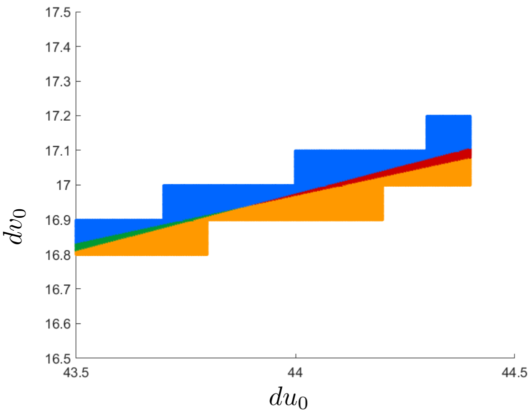

(a) Solution v^5 in $du_0 - dv_0$ diagram.

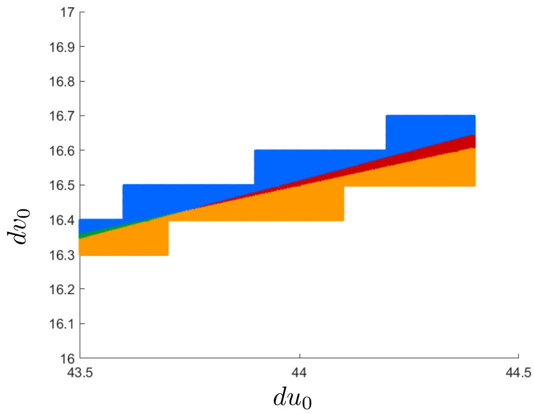

(b) Solution v^{10} in $du_0 - dv_0$ diagram.

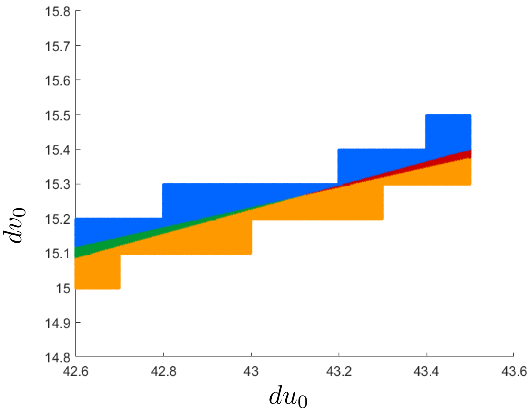

(c) Solution v^{20} in $du_0 - dv_0$ diagram.

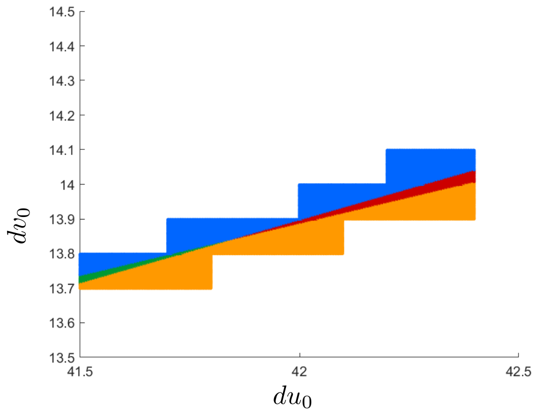

(d) Solution v^{30} in $du_0 - dv_0$ diagram.

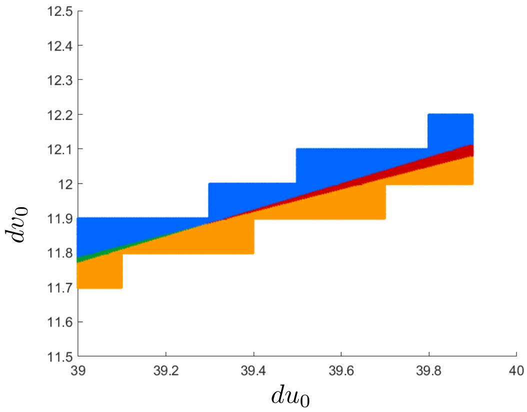

(e) Solution v^{40} in $du_0 - dv_0$ diagram.

Fig. A1: Solutions from upper branch of the bifurcation diagram shown in $du_0 - dv_0$ diagram.

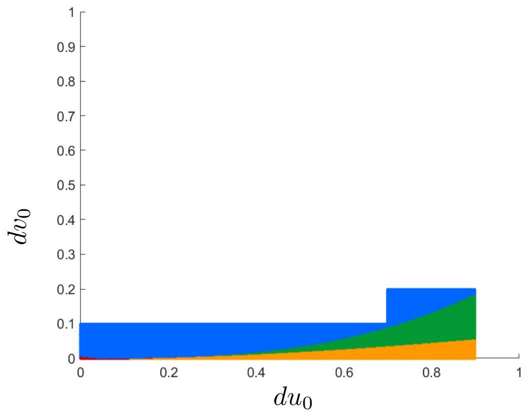

(a) Solution v_5 in $du_0 - dv_0$ diagram.

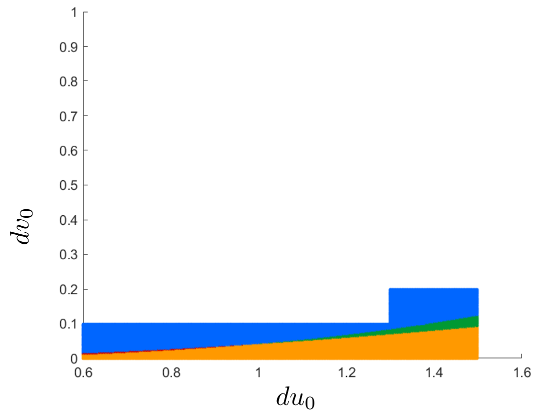

(b) Solution v_{10} in $du_0 - dv_0$ diagram.

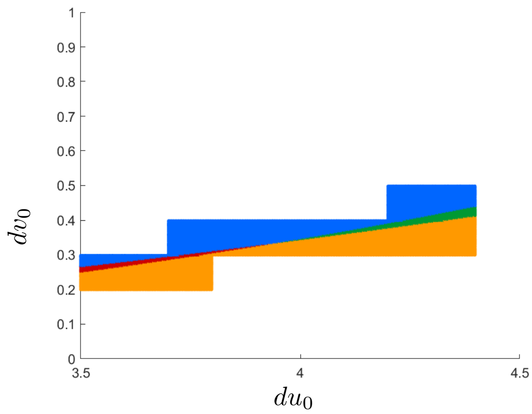

(c) Solution v_{20} in $du_0 - dv_0$ diagram.

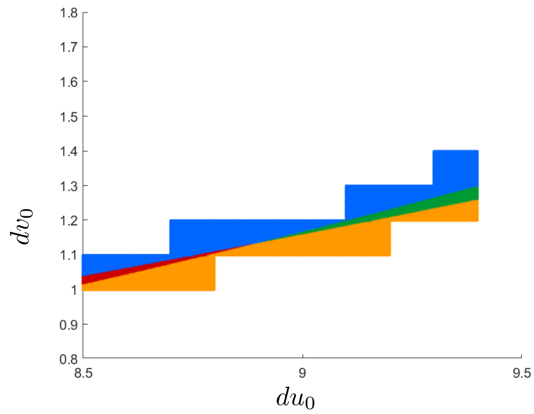

(d) Solution v_{30} in $du_0 - dv_0$ diagram.

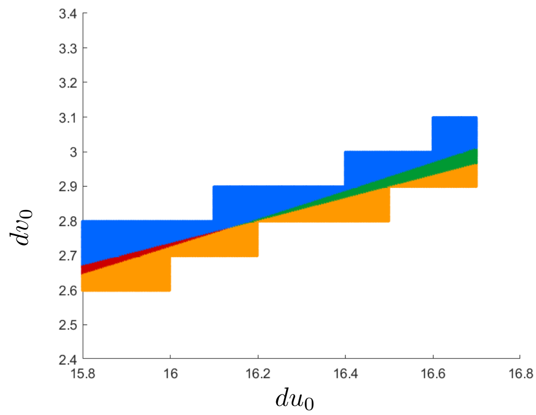

(e) Solution v_{40} in $du_0 - dv_0$ diagram.

Fig. A2: Solutions from lower branch of the bifurcation diagram shown in $du_0 - dv_0$ diagram

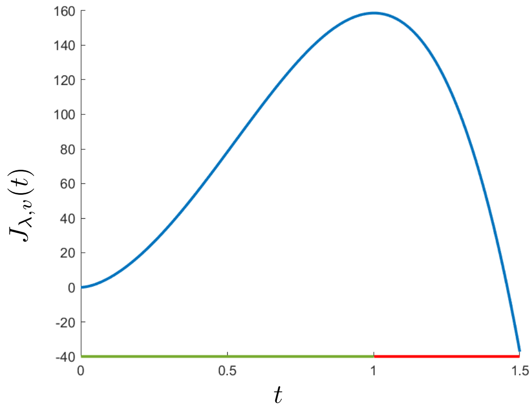

(a) J_{λ,v^λ} for $\lambda = 1$

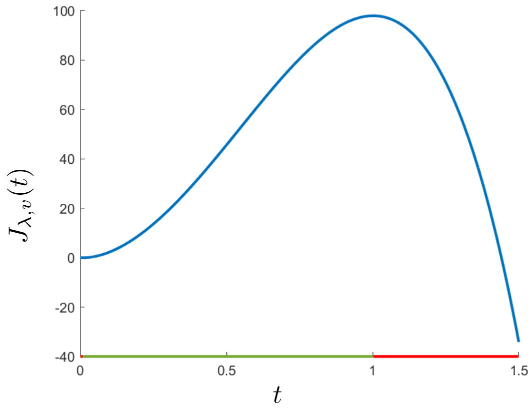

(b) J_{λ,v^λ} for $\lambda = 15$.

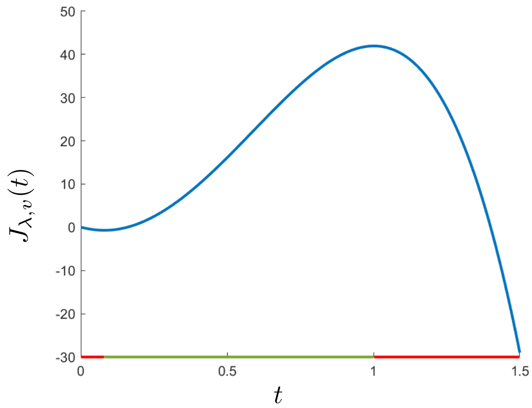

(c) J_{λ,v^λ} for $\lambda = 30$

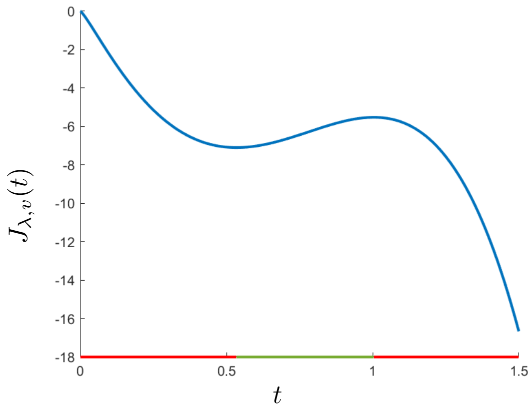

(d) J_{λ,v^λ} for $\lambda = 47$.

Fig. A3: J_{λ,v^λ} for several values of λ.

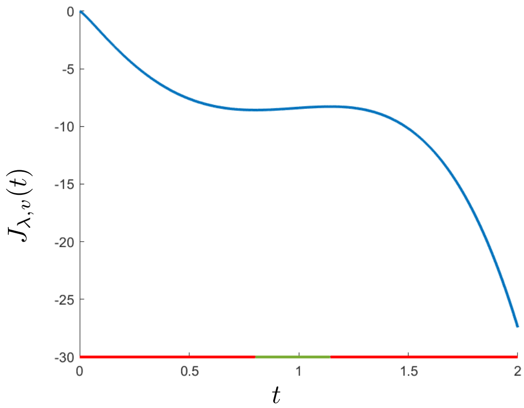

(a) J_{λ,v_λ} for $\lambda = 48.975$

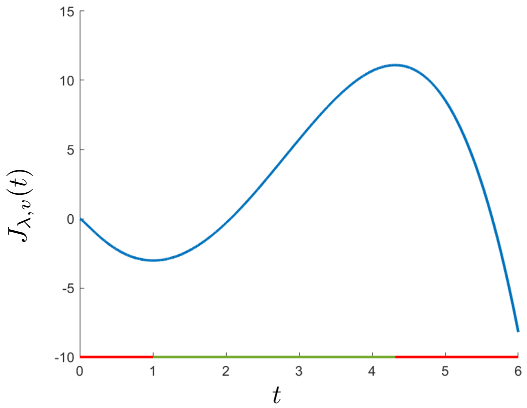

(b) J_{λ,v_λ} for $\lambda = 40$

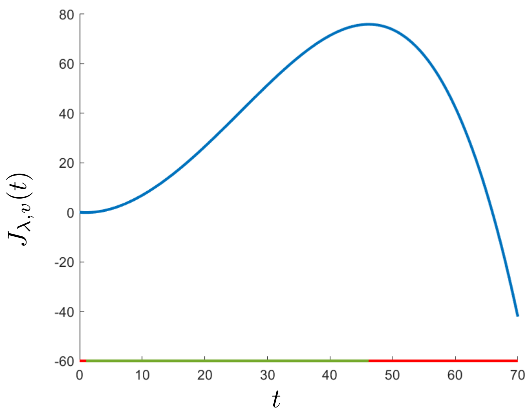

(c) J_{λ,v_λ} for $\lambda = 20$.

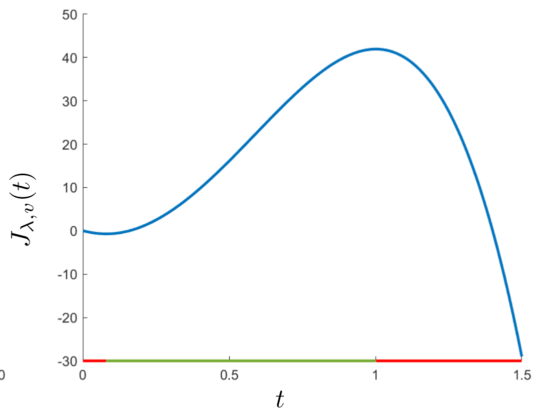

(d) J_{λ,v_λ} for $\lambda = 15$

Fig. A4: J_{λ,v_λ} for several values of λ.

Bibliography

[1] R. A. Adams and J. J. Fournier. *Sobolev spaces.* Elsevier, second edition, 2003.

[2] A. Ambrosetti, H. Brezis, and G. Cerami. Combined effects of concave and convex nonlinearities in some elliptic problems. *J. Funct. Anal.*, 122(2):519–543, 1994.

[3] J. Benedikt. Estimates of the principal eigenvalue of the p-laplacian and the p-biharmonic operator. *Mathematica Bohemica*, 140(2):215–222, 2015.

[4] H. Brezis. *Functional Analysis, Sobolev Spaces and Partial Differential Equations.* Springer, 2011.

[5] S. Chandrasekhar. *An introduction to the study of stellar structure.* The University of Chicago Press, 1939.

[6] E. M. dos Santos. On a fourth-order quasilinear elliptic equation of concave-convex type. *NoDEA Nonlinear Differential Equations Appl.*, 2009.

[7] P. Drábek and J. Milota. *Methods of nonlinear analysis: applications to differential equations.* Springer Science & Business Media, 2007.

[8] L. C. Evans. *Partial differential equations*, volume 19. American Mathematical Soc., 2010.

[9] S. Fučík and A. Kufner. *Nonlinear differential equations.* Elsevier, 1980.

[10] R. Kippenhaln and A. Weigert. *Stellar structure and evolution.* Springer-Verlag, 1990.

[11] M. Kudláč. Multi-parameter nonlinear boundary value problem. Bachelor's thesis, Západočeská univerzita v Plzni, 2021.

[12] M. Struwe. *Variational methods*, volume 34. Springer, fourth edition, 2008.

[13] V. A. Zorich. *Mathematical Analysis 1.* Springer, 2004.